Scientific African 31 (2026) e03161

Contents lists available at ScienceDirect

Scientific African

journal homepage: www.elsevier.com/locate/sciaf

Modeling and optimal control of rotavirus transmission dynamics with cost effectiveness

Jeremiah January [b,c,*], Gasper Mwanga [a], Isack E. Kibona [b], Nyimvua Shaban Mbare [c]

[a] Dar es Salaam University College of Education, University of Dar es Salaam, Tanzania
[b] Department of Mathematics and Statistics, Mbeya University of Science and Technology, Tanzania
[c] Department of Mathematics, University of Dar es Salaam, Tanzania

ARTICLE INFO

Editor name: B. Gyampoh

Keywords:
Rotavirus
Vaccination
Optimal control
Public education
Water treatment
Effective reproduction number
Hygienic practices
Cost-effectiveness

ABSTRACT

An optimal control model for rotavirus transmission was formulated to minimize both the cost of implementing interventions and the burden of infection among children and caregivers. The model integrates five time-dependent control functions: vaccination of children (u_1), public health education (u_2), treatment of infected children (u_3), water treatment and sanitation (u_4), and hygiene promotion (u_5). Pontryagin's Maximum Principle was applied to derive the necessary conditions for optimality, and numerical simulations were conducted using the Runge–Kutta method to determine the optimal time-dependent control profiles and corresponding epidemiological outcomes. Simulation results at $t = 220$ days indicate a substantial reduction in rotavirus infections among children and caregivers when integrated controls are applied. The number of infected and hospitalized children (I_b and H_b) approach zero, while the vaccinated population (V_b) reaches approximately 2.58×10^7, confirming the central role of vaccination in suppressing new infections. The concentration of environmental rotavirus particles (C_r) also tends to zero, highlighting the combined efficacy of hygiene and sanitation interventions in reducing environmental transmission. Among the evaluated control strategies, the combination of vaccination, treatment, and hygiene (S_{13}) emerges as both the most cost-effective and epidemiologically impactful strategy. This approach achieves near-complete elimination of child infections at a moderate total cost of approximately $\$6.17\times10^{11}$, yielding the best balance between health outcomes and economic feasibility. In contrast, the single-control strategies (S_1–S_5) achieve minimal infection reduction despite lower costs, while multi-control strategies involving all five interventions (S_{17}) provide marginal epidemiological improvement at substantially higher cost. The cost-effectiveness analysis, expressed as cost per health unit reduced, identifies vaccination (u_1) and treatment (u_3) as the primary contributors to financial cost, while hygiene adherence (u_5), sanitation (u_4), and education (u_2) offer strong epidemiological benefits with minimal marginal cost. This demonstrates that optimal disease control is achieved when vaccination and treatment are combined with sustained hygiene practices rather than through expensive full scale interventions. Overall, the results confirm that targeted multi control strategies particularly S_{13}p rovide the most practical and sustainable pathway for reducing rotavirus transmission, minimizing infections, and optimizing public health expenditure.

* Corresponding author at: Department of Mathematics and Statistics, Mbeya University of Science and Technology, Tanzania.
E-mail address: jruhere@gmail.com (J. January).

https://doi.org/10.1016/j.sciaf.2025.e03161
Received 3 May 2025; Received in revised form 21 November 2025; Accepted 29 December 2025
Available online 2 January 2026

Introduction

Rotavirus is a highly contagious viral disease that primarily affects infants and young children, causing severe gastroenteritis characterized by diarrhea, vomiting, fever, and dehydration [1]. The disease is responsible for a significant number of hospitalizations and deaths worldwide, particularly in low-resource settings [2]. Transmission occurs through the fecal–oral route, with contaminated hands, surfaces, food, and water acting as primary vectors of infection [3]. Rotavirus infections are most prevalent in regions with inadequate sanitation and limited access to clean water [4]. The virus spreads rapidly among children in communal settings such as daycare centers and schools, exacerbating the public health burden [5].

The most effective preventive measure is child vaccination, which has been shown to significantly reduce the incidence of severe rotavirus infections and related hospitalizations [4,5]. However, vaccine coverage must be complemented by additional strategies, including public health education, treatment of infected children, and environmental sanitation through water treatment and hygiene interventions [6].

The clinical progression of rotavirus disease varies in severity, ranging from mild diarrhea to severe dehydration that can be fatal if left untreated [7]. The primary symptoms include frequent watery diarrhea, vomiting, fever, and abdominal pain [8]. In severe cases, dehydration may lead to lethargy, sunken eyes, dry mouth, and reduced urination, necessitating urgent medical intervention [9]. Treatment is mainly supportive, focusing on oral rehydration therapy (ORT) to replenish lost fluids and electrolytes, along with zinc supplementation to reduce the duration and severity of diarrhea [10]. In more serious cases, intravenous fluid administration may be required [11]. Prompt treatment of infected children is essential to minimize complications and reduce disease transmission [12].

Despite the availability of effective vaccines, rotavirus remains a major public health concern due to gaps in vaccine coverage and variability in vaccine efficacy across populations [13]. However, existing dynamical models that incorporate caregivers' roles in disease control remain limited. Most previous mathematical models [12,14,15] examined the transmission dynamics and control strategies of rotavirus without integrating public health education among caregivers and children's hygiene behavior into the transmission process. In this paper, we apply Pontryagin's Maximum Principle, following approaches used by previous researchers [15–17], to analyze the necessary and sufficient conditions for optimal control solutions. Numerical simulations employing the fourth-order Runge–Kutta scheme demonstrate the combined effects of vaccination, public health education, treatment, environmental sanitation, and hygiene interventions in mitigating infection rates.

Cost-effectiveness analyses have shown that environmental sanitation and hygiene interventions are among the most efficient strategies for controlling rotavirus in resource-limited settings [18]. Findings by researchers [15] indicate that vaccination is the most effective strategy, followed by health education and treatment. Results from related studies [12,14,17] highlight the need for integrated control strategies that prioritize child vaccination while reinforcing sanitation and hygiene practices. Despite advancements in vaccination and control measures, rotavirus continues to impose a significant health and economic burden globally [19]. Strengthening existing interventions and developing innovative strategies for rotavirus prevention remain crucial to reducing rotavirus-related morbidity and mortality [20].

In addition to vaccination, sustained investment in water, sanitation, and hygiene (WASH) initiatives is vital for reducing the overall burden of rotavirus disease [21]. Community-level engagement and awareness campaigns can empower individuals to adopt better hygiene practices, further decreasing transmission rates [22]. Governments and health organizations should work collaboratively to implement comprehensive intervention programs that integrate both medical and environmental strategies [23, 24].

Furthermore, continued surveillance and monitoring of rotavirus epidemiology are essential for assessing the impact of control measures and identifying emerging challenges [25]. Advances in diagnostic technologies can aid early detection and rapid response to outbreaks, ensuring effective disease management [26]. This study focuses on optimizing intervention strategies that are both accessible and affordable in vulnerable communities of developing countries, particularly Tanzania. Research into next-generation vaccines with improved efficacy and durability could further enhance global control efforts. Ultimately, a multifaceted approach combining vaccination, public health education, treatment, environmental sanitation, and hygiene interventions is vital to reducing the global burden of rotavirus [27]. This article aims to determine the optimal and cost-effective combination of child vaccination, caregiver education, treatment, and hygiene practices to achieve sustainable disease control. By addressing both medical and environmental determinants of transmission, policymakers and health professionals can work toward lasting control and prevention of this devastating illness.

Formulation of the optimal control model for rotavirus transmission

In this study, we develop an optimal control problem to reduce rotavirus transmission among children under five years of age and their caregivers, while accounting for the cost-effectiveness of five intervention strategies. The total population is divided into two groups: children $N_b(t)$ and caregivers $N_a(t)$, with children categorized into susceptible $S_b(t)$, vaccinated $V_b(t)$, infected $I_b(t)$, hospitalized $H_b(t)$, and recovered $R_b(t)$, and caregivers into susceptible $S_a(t)$, paratenic hosts $P_a(t)$, and infected $I_a(t)$. Environmental contamination is represented by the compartment $C_r(t)$, which accumulates viral particles from infected children, caregivers, and paratenic hosts at rates $\omega_1, \omega_2, \omega_3$, respectively, and clears naturally at rate μ_r, or through sanitation at rate $\rho(1+u_4(t))$. Children and individuals above five years enter the system at rates π_b and π_a, and exit at natural death rates μ_b and μ_a, respectively. Transmission

occurs via direct and environmental routes, with the force of infection for children α_b and caregivers α_a defined by the following equation:

$$\begin{aligned}\alpha_b &= \frac{\beta_b(1-h_1(1+u_5))I_b}{N_b} + \frac{\phi_1(1-h_1(1+u_5))C_r}{\nu+C_r} + \frac{(1-\varepsilon_a(1+u_2))(\phi_2 I_a+\phi_3 P_a)}{N_a},\\ \alpha_a &= \frac{\xi_1(1-\varepsilon_a(1+u_2))C_r}{\nu+C_r} + \frac{\xi_2(1-h_1(1+u_5))I_b}{N_b},\end{aligned} \tag{1}$$

incorporating hygiene and public health controls. Children may be vaccinated at rate $\eta(1+u_1(t))$, with vaccine efficacy $\kappa \in [0,1]$. Infection may lead to recovery at rate γ_b, hospitalization at rate $\tau(1+u_3(t))$, or death either at home δ_1 or in hospital δ_2, with hospitalized children recovering at rate χ_b. Caregivers infected through contact with infected children or contaminated environments, at rates ξ_1 and ξ_2, move from susceptible to paratenic hosts at rate α_a, then progress to the infectious class at rate $\beta_a(1-\varepsilon_a(1+u_2(t)))$. Hygiene practices among children reduce transmission by $1-h_1(1+u_5(t))$, while caregiver education reduces susceptibility by $1-\varepsilon_a(1+u_2(t))$. The optimal model is formulated by introducing five time-dependent control strategies: $u_1(t)$, representing vaccination efforts for susceptible children; $u_2(t)$, representing public health education efforts for caregivers; $u_3(t)$, representing treatment efforts for infected children; $u_4(t)$, denoting sanitation and water treatment efforts to reduce environmental contamination; and $u_5(t)$, representing hygiene practice efforts among children. For convenience, $u_i(t)$ will be referred to as u_i, where $i = 1,2,3,4,5$. The controlled system of ordinary differential equations (ODEs) is given as follows:

$$\begin{cases}
\frac{dS_b}{dt} = \pi_b - \alpha_b S_b - (\eta(1+u_1)+\mu_b)S_b\\
\frac{dV_b}{dt} = \eta(1+u_1)S_b - \mu_b V_b - \alpha_b(1-\kappa)V_b\\
\frac{dI_b}{dt} = \alpha_b S_b + \alpha_b(1-\kappa)V_b - (\mu_b+\delta_1+\gamma_b+\tau(1+u_3))I_b\\
\frac{dH_b}{dt} = \tau(1+u_3)I_b - (\mu_b+\delta_2+\chi_b)H_b\\
\frac{dR_b}{dt} = \gamma_b I_b + \chi_b H_b - \mu_b R_b\\
\frac{dC_r}{dt} = \omega_1(1-h_1(1+u_5))I_b + \omega_3(1-\varepsilon_a(1+u_2))P_a + \omega_2(1-\varepsilon_a(1+u_2))I_a - (\mu_r+\rho(1+u_4))C_r\\
\frac{dS_a}{dt} = \pi_a - \alpha_a S_a - \mu_a S_a\\
\frac{dP_a}{dt} = \alpha_a S_a - \beta_a(1-\varepsilon_a(1+u_2))P_a - \mu_a P_a\\
\frac{dI_a}{dt} = \beta_a(1-\varepsilon_a(1+u_2))P_a - \mu_a I_a
\end{cases} \tag{2}$$

with corresponding initial conditions specifying the initial number of individuals in each compartment given as :

$$\begin{aligned}S_b(0) = S_{b0} \geq 0,\ V_b(0) = V_{b0} \geq 0,\ I_b(0) = I_{b0} \geq 0,\ H_b(0) = H_{b0} \geq 0,\ R_b(0) = R_{b0} \geq 0,\\ C_r(0) = C_{r0} \geq 0,\ S_a(0) = S_{a0} \geq 0,\ P_a(0) = P_{a0} \geq 0,\ I_a(0) = I_{a0} \geq 0\end{aligned}$$

To determine the optimal level of intervention strategies required to control rotavirus disease, we first formulate the objective function $J(u_i)$ for system of Eq. (2). The goal is to minimize the number of infections over a given time period T among children, caregivers, and environmental reservoirs, as well as to reduce the cost associated with the control strategies. The objective functional to be minimized is given by:

$$J(u_1,u_2,u_3,u_4,u_5) = \int_0^T \left(B_1 I_b(t) + B_2 I_a(t) + B_3 H_b(t) + B_4 C_r(t) + \frac{c_1}{2}u_1^2 + \frac{c_2}{2}u_2^2 + \frac{c_3}{2}u_3^2 + \frac{c_4}{2}u_4^2 + \frac{c_5}{2}u_5^2\right) dt, \tag{3}$$

subject to the differential equations in system of Eq. (1), where T is the final time. The term $\sum_{i=1}^{5} \frac{c_i}{2}u_i^2$ represents the cost associated with the control strategies u_i for $i = 1,2,3,4,5$, where c_i are positive weight constants that measure the relative costs of implementing each intervention. The parameters B_1, B_2, B_3, and B_4 are positive weight constants corresponding to infected children, infected caregivers, hospitalized children, and rotavirus concentration in the environment, respectively. The intervention costs are expressed in quadratic form to reflect the nonlinear nature of cost functions.

Thus, we need to determine numerically the optimal control strategies $\{u_1^*, u_2^*, u_3^*, u_4^*, u_5^*\}$ such that;

$$J(u_1^*,u_2^*,u_3^*,u_4^*,u_5^*) = \min J(u_1,u_2,u_3,u_4,u_5) \quad \text{for} \quad (u_1,u_2,u_3,u_4,u_5) \in \Pi,$$

where the control set Π is Lebesgue measurable and defined as;

$$\Pi = \{(u_1,u_2,u_3,u_4,u_5) \mid 0 \leq u_i \leq 1, \quad i = 1,2,3,4,5, \quad \forall t \in [0,T]\}.$$

The control constraints are:

$$0 \leq u_1(t), u_2(t), u_3(t), u_4(t), u_5(t) \leq 1.$$

Existence of the optimal control

An optimal control problem for system (2) exists if the necessary conditions for optimality, derived using Pontryagin's Maximum Principle, are satisfied. Specifically, the optimal control solutions

$$J(u_1^*, u_2^*, u_3^*, u_4^*, u_5^*) = \min_{(u_1,u_2,u_3,u_4,u_5)\in \Pi} J(u_1, u_2, u_3, u_4, u_5)$$

must hold. However, the existence of an optimal control is not always guaranteed; therefore, it is essential to verify that the problem admits a solution before attempting to compute the optimal control. In this work, we use Fleming and Rishel's approach to establish the existence of an optimal control [28].

Consider the system of ODEs (2) governing the transmission dynamics of rotavirus among children, caregivers, and their environment. The corresponding objective functional $J(U)$, defined in (3), is to be minimized. To establish the existence of an optimal control, we verify the standard assumptions of Fleming and Rishel for our system. First, the system function

$$F(t, X, U) = \big(F_1(t, X, U), \ldots, F_9(t, X, U)\big),$$

which defines the ODEs for the state variables $S_b, V_b, I_b, H_b, R_b, C_r, S_a, P_a, I_a$, is continuous in t, X, and U. Moreover, F satisfies a Lipschitz condition with respect to the state and control variables; that is, there exists a constant $L > 0$ such that for all X_1, X_2 and U_1, U_2,

$$\|F(t, X_1, U_1) - F(t, X_2, U_2)\| \le L\big(\|X_1 - X_2\| + \|U_1 - U_2\|\big), \quad \forall\, t \in [0, T], \tag{4}$$

ensuring well-posedness of the system.

The control set is defined by

$$\Pi = \left\{(u_1, u_2, u_3, u_4, u_5) \mid 0 \le u_i(t) \le 1,\ \forall t \in [0, T]\right\}, \tag{5}$$

which is convex and closed.

The system satisfies the bounded growth condition: there exists $M > 0$ such that

$$\|F(t, X, U)\| \le M\big(1 + \|X\| + \|U\|\big), \tag{6}$$

ensuring that solutions do not blow up in finite time and remain bounded for all $t \in [0, T]$.

The objective functional $J(U)$ is convex with respect to the control variables and satisfies a lower bound

$$J(U) \ge k_1\Big(|u_1|^2 + |u_2|^2 + |u_3|^2 + |u_4|^2 + |u_5|^2\Big)^{\xi/2} - k_2, \tag{7}$$

for some constants $k_1, k_2 > 0$ and $\xi > 1$. This ensures the functional cannot decrease without bound.

By verifying these conditions for (2), Fleming and Rishel's theorem guarantees the existence of an optimal control. Therefore, there exists a control vector

$$U^* = (u_1^*, u_2^*, u_3^*, u_4^*, u_5^*) \in \Pi$$

that minimizes $J(U)$, with the corresponding state trajectories absolutely continuous on $[0, T]$.

Theorem 1 (*Existence of Optimal Control for the Rotavirus Model* (2))**.** *For the optimal control problem associated with system* (2)*, there exists an optimal control vector*

$$U^* = (u_1^*, u_2^*, u_3^*, u_4^*, u_5^*) \in \Pi$$

such that

$$J(u_1^*, u_2^*, u_3^*, u_4^*, u_5^*) = \min_{(u_1,u_2,u_3,u_4,u_5)\in \Pi} J(u_1, u_2, u_3, u_4, u_5).$$

Proof. We consider the controlled rotavirus model described by

$$\dot{X}(t) = F(t, X(t), U(t)), \quad X(0) = X_0,$$

where

$$X(t) = (S_b, V_b, I_b, H_b, R_b, C_r, S_a, P_a, I_a)^\top$$

and

$$U(t) = (u_1(t), u_2(t), u_3(t), u_4(t), u_5(t))^\top.$$

The system satisfies continuity and Lipschitz conditions as discussed above.

All state variables remain non-negative and uniformly bounded for all admissible controls. Therefore, the right-hand side of (2) is finite for all $t \in [0,T]$. Furthermore, each function $F_i(t,X,U)$ is continuously differentiable, ensuring the existence of an $L > 0$ such that

$$\|F(t,X_1,U_1) - F(t,X_2,U_2)\| \le L(\|X_1 - X_2\| + \|U_1 - U_2\|).$$

The control set Π is convex and closed, and the bounded-growth condition is satisfied:

$$\|F(t,X,U)\| \le M(1 + \|X\| + \|U\|).$$

The objective functional is convex in the controls and coercive:

$$J(U) \ge k_1 \left(|u_1|^2 + |u_2|^2 + |u_3|^2 + |u_4|^2 + |u_5|^2\right)^{\xi/2} - k_2.$$

Hence, all the hypotheses of Fleming and Rishel's theorem are satisfied for the rotavirus control system defined in Eq. (2). Specifically, the existence of admissible state-control pairs, convexity and closure of the control set, Lipschitz continuity and boundedness of the right-hand side, convexity of the objective functional, and coercivity of the cost integrand guarantee the existence of an optimal control $U^* = (u_1^*, u_2^*, u_3^*, u_4^*, u_5^*) \in \Pi$. Therefore, there exists an optimal control that minimizes the functional $J(U)$ and generates corresponding absolutely continuous state trajectories $X^*(t)$ satisfying the rotavirus system (2) with initial condition $X^*(0) = X_0$. This establishes the existence of an optimal control for the rotavirus model system (2). □

Following Lukes' theorem as applied in [29], we formally state the existence result.

Theorem 2 (*Lukes' Theorem Applied to the Rotavirus Modelsystem* (2))**.** *Let the controlled rotavirus system be given by* (2)

$$\dot{X}(t) = F(t, X(t), U(t)), \qquad X(0) = X_0,$$

with state vector

$$X(t) = (S_b, V_b, I_b, H_b, R_b, C_r, S_a, P_a, I_a)^\top$$

and control vector

$$U(t) = (u_1, u_2, u_3, u_4, u_5)^\top \in \Pi,$$

where the admissible control set is

$$\Pi = \{U(\cdot) : [0,T] \to [0,1]^5\}.$$

Assume that the model parameters (e.g. $\pi_b, \pi_a, \mu_b, \mu_a, \eta, \gamma_b, \tau, \chi_b, \delta_1, \delta_2, \omega_i, \mu_r, \rho, \beta_b, \xi_i, \phi_j, \kappa, \nu, c_i, B_j$*) are non-negative and finite, and that the initial state* X_0 *is non-negative. If the following hold:*

(i) The right-hand side $F(t,X,U)$ *is continuous in* t *and continuously differentiable in* (X,U) *for admissible* (X,U) *(hence locally Lipschitz in* X *and* U*);*

(ii) The state components are non-negative and admit uniform upper bounds (biological bounds) so that

$$0 \le S_b, V_b, I_b, H_b, R_b \le N_b, \qquad 0 \le S_a, P_a, I_a \le N_a, \qquad 0 \le C_r \le C_{\max};$$

(iii) F *satisfies a linear growth bound in* (X,U)*, i.e. there exists* $M > 0$ *s.t.*

$$\|F(t,X,U)\| \le M\left(1 + \|X\| + \|U\|\right) \quad \text{for all admissible } (t,X,U);$$

(iv) The admissible control set Π *is convex and closed (indeed* $\Pi = [0,1]^5$ *pointwise);*

(v) The cost integrand in the objective functional (3) *is convex in the controls and the objective functional is bounded below,*

then there exists an optimal control

$$U^* = (u_1^*, u_2^*, u_3^*, u_4^*, u_5^*) \in \Pi$$

and an associated absolutely continuous state trajectory $X^*(\cdot)$ *on* $[0,T]$ *which together minimize the cost* $J(U)$*.*

Proof. The proof verifies the hypotheses of Lukes' existence result in the concrete setting of system (2) and then invokes the theorem to conclude existence of an optimal control.

First, by inspection of (2) each component of F is built from polynomial, rational (of the form $C_r/(\nu + C_r)$) and bilinear terms in state and control variables multiplied by non-negative parameters (for example transmission terms $\beta_b(1 - h_1(1 + u_5))I_b/N_b$, environmental contributions $\phi_1(1 - h_1(1 + u_5))C_r/(\nu + C_r)$, accumulation terms $\omega_i(\cdot)$, and linear removal terms $(\mu_r + \rho(1 + u_4))C_r$). With the hypothesis that all parameters are finite and non-negative and that the controls satisfy $0 \le u_i \le 1$, these expressions are continuous in t (parameters are time-independent here), and continuously differentiable in (X,U) for admissible values of X and U. Hence condition (1) (continuity and differentiability) holds and local Lipschitz continuity follows from differentiability. Second, non-negativity of solutions is enforced by the epidemiological structure: recruitment terms (π_b, π_a) are non-negative and every outflow term from a compartment is proportional to the compartment size or a non-negative rate. Standard comparison/positivity arguments

for compartmental models (Gronwall-type estimates or inspection of differential inequalities obtained by removing nonnegative inflows) yield that, given non-negative initial data X_0, each compartment remains non-negative for all $t \geq 0$. Uniform upper bounds follow from simple balance estimates: for example the total child population satisfies;

$$\frac{dN_b}{dt} \leq \pi_b - \mu_b N_b \quad \Rightarrow \quad N_b(t) \leq \frac{\pi_b}{\mu_b},$$

so that $S_b, V_b, I_b, H_b, R_b \leq N_b(t) \leq \pi_b/\mu_b$. Analogous bounds hold for caregiver compartments $N_a(t) \leq \pi_a/\mu_a$. For the environmental load one obtains from (2) (sixth equation) the inequality

$$\frac{dC_r}{dt} \leq (\omega_1 + \omega_2 + \omega_3)\max(I_b, I_a, P_a) - (\mu_r + \rho)C_r,$$

so at equilibrium $C_r \leq (\omega_1 I_b + \omega_2 I_a + \omega_3 P_a)/(\mu_r + \rho) \leq (\omega_1 + \omega_2 + \omega_3)\max(N_b, N_a)/(\mu_r + \rho)$; set this right-hand side to define $C_{\max}$. Thus condition (2) (existence of uniform biological bounds) is satisfied.

Third, since each F_i is composed of sums and products of bounded state and control components with finite parameters, there exists a constant $M > 0$ such that for admissible (X, U)

$$|F_i(t, X, U)| \leq M\big(1 + \|X\| + \|U\|\big), \qquad i = 1, \ldots, 9,$$

and therefore $\|F(t, X, U)\| \leq M(1 + \|X\| + \|U\|)$. This verifies the linear growth bound (condition (3)). Combined with continuous differentiability, the linear growth and bounded domain imply a global Lipschitz constant $L > 0$ on the admissible set so that for any admissible (X_1, U_1) and (X_2, U_2)

$$\|F(t, X_1, U_1) - F(t, X_2, U_2)\| \leq L\big(\|X_1 - X_2\| + \|U_1 - U_2\|\big),$$

establishing the Lipschitz property used in Lukes' framework.

Fourth, the control set $\Pi = [0, 1]^5$ (pointwise in time) is closed and convex by construction; convexity follows because each admissible control is a vector of values in a convex interval and pointwise convex combinations remain admissible. Hence condition (4) holds.

Fifth, the objective integrand from Eq. (3) with $c_i > 0$ by model design. This integrand is convex in u (sum of positive quadratics) and measurable in t; moreover the integral is bounded below (nonnegative linear state terms plus nonnegative quadratic control terms) and satisfies the coercivity/lower-bound condition assumed in Lukes' theorem (there exist $k_1, k_2 > 0$, $\xi > 1$ with $J(U) \geq k_1\|u\|^\xi - k_2$ on Π because of the quadratic control penalties). Therefore the cost functional is convex and lower bounded, verifying condition (5).

With all hypotheses of Lukes' existence theorem satisfied on the admissible set (continuity and differentiability of F, Lipschitz property, linear growth, boundedness and non-negativity of states, convex closed control set, convex and coercive cost), the theorem guarantees the existence of an optimal control $U^* \in \Pi$ and an associated absolutely continuous state trajectory $X^*(\cdot)$ on $[0, T]$ which minimize $J(U)$. Moreover, for any admissible control the state system admits a unique solution by the Lipschitz property, and the minimizing sequence of controls has a convergent subsequence (weakly in L^2) whose limit is admissible and attains the infimum due to lower semicontinuity of the convex cost; these standard arguments (compactness, weak lower semicontinuity, and direct method in the calculus of variations) complete the construction of the minimizer in the Lukes framework.

Thus Lukes' theorem (as applied in [29]) yields existence of an optimal control for the rotavirus model (2) given the stated assumptions on parameters and admissible controls. □

Characterization of the optimal control

Pontryagin's Maximum Principle is applied to establish the necessary conditions that an optimal control strategy must satisfy and to solve the optimal control problem. This principle transforms the system of Eqs. (2) and the objective fuction Eq. (3) into an equivalent problem of minimizing a piecewise-defined Hamiltonian function H with respect to the control variables u_1, u_2, u_3, u_4, and u_5, such that the corresponding Hamiltonian function is formulated as:

$$H = B_1 I_b + B_2 H_b + B_3 C_r + B_4 I_a + \sum_{i=1}^{5} \frac{c_i}{2} u_i^2 + \sum_{i=1}^{9} \lambda_i f_i, \tag{8}$$

where each f_j corresponds to the right hand side of the state equations, and λ_j are the adjoint variables and the term $\sum_{i=1}^{9} \lambda_i f_i$ captures the influence of each state variable on the objective functional. Hence, the Hamiltonian function incorporates both (cost) terms and the system dynamics via the adjoint variables and the Lagrangian function is defined as:

$$L(I_b, H_b, C_r, I_a, u_1, u_2, u_3, u_4, u_5, t) = B_1 I_b + B_2 H_b + B_3 C_r + B_4 I_a + \frac{1}{2}c_1 u_1^2 + \frac{1}{2}c_2 u_2^2 + \frac{1}{2}c_3 u_3^2 + \frac{1}{2}c_4 u_4^2 + \frac{1}{2}c_5 u_5^2.$$

Here, λ_j for $j = 1, 2, \ldots, 9$ are the adjoint variables that must be determined using Pontryagin's Maximum Principle. The expanded form of the Hamiltonian function in Eq. (8) is given as follows:

$$\begin{aligned} H = {} & L(I_b, H_b, C_r, I_a, u_1, u_2, u_3, u_4, u_5, t) \\ & + \lambda_1 \left(\pi_b - \alpha_b S_b - (\eta(1+u_1) + \mu_b) S_b\right) \\ & + \lambda_2 \left(\eta(1+u_1) S_b - \mu_b V_b - \alpha_b (1-\kappa) V_b\right) \\ & + \lambda_3 \left(\alpha_b S_b + \alpha_b (1-\kappa) V_b - (\mu_b + \delta_1 + \gamma_b + \tau(1+u_3)) I_b\right) \\ & + \lambda_4 \left(\tau(1+u_3) I_b - (\mu_b + \delta_2 + \chi_b) H_b\right) \\ & + \lambda_5 \left(\gamma_b I_b + \chi_b H_b - \mu_b R_b\right) \\ & + \lambda_6 \left(\omega_1 (1 - h_1(1+u_5)) I_b + \omega_3 (1 - \varepsilon_a (1+u_2)) P_a + \omega_2 (1 - \varepsilon_a (1+u_2)) I_a - (\mu_r + \rho(1+u_4)) C_r\right) \\ & + \lambda_7 \left(\pi_a - \alpha_a S_a - \mu_a S_a\right) \\ & + \lambda_8 \left(\alpha_a S_a - \beta_a (1 - \varepsilon_a (1+u_2)) P_a - \mu_a P_a\right) \\ & + \lambda_9 \left(\beta_a (1 - \varepsilon_a (1+u_2)) P_a - \mu_a I_a\right). \end{aligned} \tag{9}$$

To determine the optimal control strategy, we employ *Pontryagin's Maximum Principle*, which provides necessary conditions for optimality.

Theorem 3 (*Necessary Conditions via Pontryagin's Maximum Principle*)**.** *Consider the controlled rotavirus system (2) with state vector*

$$X(t) = (S_b, V_b, I_b, H_b, R_b, C_r, S_a, P_a, I_a)^\top$$

and control vector

$$U(t) = (u_1, u_2, u_3, u_4, u_5)^\top \in \mathcal{U} = \{\, U : [0,T] \to [0,1]^5 \,\}.$$

Let the objective functional be given by (3). Assume all model parameters are nonnegative and finite, and that the initial state satisfies $X(0) = X_0 \geq 0$.

Then any optimal control $U^*(t)$ *and the corresponding optimal trajectory* $X^*(t)$ *satisfy the Pontryagin Maximum Principle: there exist absolutely continuous adjoint (costate) functions* $\lambda_i(t)$, $i = 1, \ldots, 9$, *such that*

$$\dot{\lambda}_i(t) = -\frac{\partial H}{\partial x_i}(t), \qquad \lambda_i(T) = 0,$$

and, for almost every $t \in [0,T]$,

$$u_i^*(t) = \min\Big\{ \max\big(0,\, \hat{u}_i(t)\big),\, 1 \Big\}, \qquad i = 1, \ldots, 5,$$

where $\hat{u}_i(t)$ *denotes the unconstrained optimal control, obtained by solving the first-order necessary condition*

$$\frac{\partial H}{\partial u_i} = 0.$$

Hence, the optimal controls are expressed as

$$u_i^*(t) = -\frac{1}{c_i} \frac{\partial H}{\partial u_i}, \qquad i = 1, 2, \ldots, 5.$$

The Hamiltonian H *and the corresponding adjoint system are given explicitly below.*

Proof. We prove the theorem by (i) verifying the regularity hypotheses of PMP for our specific model, (ii) writing the Hamiltonian explicitly in model variables and parameters, (iii) deriving the adjoint system and transversality conditions, (iv) computing the control extremizers and projecting them onto $[0,1]$, and (v) giving a short biological interpretation of the adjoint variables. Regularity and hypotheses. The right-hand side of the state system (2) is formed by sums of the following types of terms: recruitment constants (e.g. π_b, π_a), linear removals (e.g. $\mu_b S_b,\ \mu_a S_a$), bilinear infection terms of the form $\beta_b(1 - h_1(1+u_5)) I_b S_b / N_b$, rational environmental terms of the form $\phi_1(1 - h_1(1+u_5)) C_r/(\nu + C_r)$, and linear control-modified rates such as $\eta(1+u_1)S_b$, $\tau(1+u_3)I_b$, and $\rho(1+u_4)C_r$. With the admissible-control constraint $0 \leq u_i \leq 1$, and positive finite parameters, each right-hand-side component is continuously differentiable in the state variables X and the controls U on the biologically admissible set $\{X \geq 0,\ N_b \leq \pi_b/\mu_b,\ N_a \leq \pi_a/\mu_a,\ C_r \leq C_{\max}\}$. Hence the local Lipschitz condition in X holds and linear growth bounds of the form

$$\|F(t, X, U)\| \leq M(1 + \|X\| + \|U\|)$$

are satisfied for some $M > 0$. These properties guarantee existence and uniqueness of the state trajectory for any admissible control and provide the differentiability needed to apply PMP.

Hamiltonian. Define the running cost (integrand) $L(X,U) = B_1 I_b + B_2 I_a + B_3 H_b + B_4 C_r + \frac{1}{2}\sum_{i=1}^5 c_i u_i^2$. The Hamiltonian is

$$H(X, U, \lambda) = L(X, U) + \sum_{i=1}^{9} \lambda_i F_i(X, U),$$

where we identify F_i with the right-hand side of the ith equation of system of (ODEs) (2). Writing the Hamiltonian in full is straightforward but lengthy; we instead give each term when needed to compute partial derivatives . By PMP the adjoint equations are $\dot{\lambda}_i = -\partial H/\partial x_i$ with terminal conditions $\lambda_i(T) = 0$. Substituting F_i and L and differentiating with respect to the state variables yields the explicit costate system that match and refine the previously stated Eq. (8) which gives:

$$
\begin{cases}
\frac{d\lambda_1}{dt} = -\frac{\partial H}{\partial S_b} = \lambda_1\big(\alpha_b + \eta(1+u_1) + \mu_b\big) - \lambda_2\eta(1+u_1) - \lambda_3\alpha_b, \\
\frac{d\lambda_2}{dt} = -\frac{\partial H}{\partial V_b} = \lambda_2\big(\mu_b + \alpha_b(1-\kappa)\big) - \lambda_3\alpha_b(1-\kappa), \\
\frac{d\lambda_3}{dt} = -\frac{\partial H}{\partial I_b} = -B_1 + (\lambda_1-\lambda_3)\frac{\partial \alpha_b}{\partial I_b}S_b + (\lambda_2-\lambda_3)\frac{\partial \alpha_b}{\partial I_b}(1-\kappa)V_b \\
\qquad + \lambda_3\big(\mu_b + \delta_1 + \gamma_b + \tau(1+u_3)\big) - \lambda_4\tau(1+u_3) - \lambda_5\gamma_b - \lambda_6\omega_1(1-h_1(1+u_5)), \\
\frac{d\lambda_4}{dt} = -\frac{\partial H}{\partial H_b} = -B_2 + \lambda_4(\mu_b + \delta_2 + \chi_b) - \lambda_5\chi_b, \\
\frac{d\lambda_5}{dt} = -\frac{\partial H}{\partial R_b} = \lambda_5\mu_b, \\
\frac{d\lambda_6}{dt} = -\frac{\partial H}{\partial C_r} = -B_3 + (\lambda_1-\lambda_3)\frac{\partial \alpha_b}{\partial C_r}S_b + (\lambda_2-\lambda_3)\frac{\partial \alpha_b}{\partial C_r}(1-\kappa)V_b \\
\qquad + \lambda_6(\mu_r + \rho(1+u_4)) - (\lambda_7-\lambda_8)\frac{\partial \alpha_a}{\partial C_r}S_a - (\lambda_9-\lambda_8)\omega_2(1-\varepsilon_a(1+u_2)), \\
\frac{d\lambda_7}{dt} = -\frac{\partial H}{\partial S_a} = \lambda_7(\alpha_a + \mu_a) - \lambda_8\alpha_a, \\
\frac{d\lambda_8}{dt} = -\frac{\partial H}{\partial P_a} = \lambda_8\big(\mu_a + \beta_a(1-\varepsilon_a(1+u_2))\big) - \lambda_9\beta_a(1-\varepsilon_a(1+u_2)), \\
\frac{d\lambda_9}{dt} = -\frac{\partial H}{\partial I_a} = -B_4 + (\lambda_3-\lambda_6)\omega_2(1-\varepsilon_a(1+u_2)) + \lambda_9\mu_a.
\end{cases}
\tag{10}
$$

Here the partial derivatives of the forces of infection used above are

$$
\frac{\partial \alpha_b}{\partial I_b} = \frac{\beta_b(1-h_1(1+u_5))}{N_b}, \qquad \frac{\partial \alpha_b}{\partial C_r} = \frac{\phi_1(1-h_1(1+u_5))\nu}{(\nu+C_r)^2},
$$

and (as previously)

$$
\frac{\partial \alpha_b}{\partial u_2} = -\frac{\varepsilon_a(\phi_2 I_a + \phi_3 P_a)}{N_a}, \qquad \frac{\partial \alpha_b}{\partial u_5} = -h_1\Big(\frac{\beta_b I_b}{N_b} + \frac{\phi_1 C_r}{\nu + C_r}\Big),
$$

while

$$
\frac{\partial \alpha_a}{\partial C_r} = \frac{\xi_1(1-\varepsilon_a(1+u_2))\nu}{(\nu+C_r)^2}.
$$

Terminal conditions are $\lambda_i(T) = 0$ for $i = 1, \ldots, 9$, consistent with the fixed terminal time and free terminal state.

Optimality conditions for controls. Differentiating H with respect to each control u_i yields the stationarity conditions. For our model these derivatives are given as:

$$
\begin{cases}
\frac{\partial H}{\partial u_1} = (\lambda_2-\lambda_1)\eta S_b + c_1u_1, \\
\frac{\partial H}{\partial u_2} = -(\lambda_1-\lambda_3)\frac{\varepsilon_a(\phi_2 I_a + \phi_3 P_a)}{N_a}S_b - (\lambda_2-\lambda_3)\frac{\varepsilon_a(\phi_2 I_a + \phi_3 P_a)}{N_a}(1-\kappa)V_b \\
\qquad +\lambda_6\varepsilon_a(\omega_3 P_a + \omega_2 I_a) + (\lambda_7-\lambda_8)\frac{\xi_1 C_r}{\nu+C_r}S_a\varepsilon_a + (\lambda_8-\lambda_9)\beta_a P_a\varepsilon_a + c_2u_2, \\
\frac{\partial H}{\partial u_3} = (\lambda_4-\lambda_3)\tau I_b + c_3u_3, \\
\frac{\partial H}{\partial u_4} = \lambda_6\rho C_r + c_4u_4, \\
\frac{\partial H}{\partial u_5} = -(\lambda_1-\lambda_3)h_1\Big(\frac{\beta_b I_b}{N_b} + \frac{\phi_1 C_r}{\nu+C_r}\Big)S_b \\
\qquad -(\lambda_2-\lambda_3)h_1\Big(\frac{\beta_b I_b}{N_b} + \frac{\phi_1 C_r}{\nu+C_r}\Big)(1-\kappa)V_b - \lambda_6\omega_1 h_1 I_b + (\lambda_7-\lambda_8)\frac{\xi_2 I_b}{N_b}S_a h_1 + c_5u_5.
\end{cases}
\tag{11}
$$

Setting these derivatives to zero (ignoring temporarily constraints) gives the unconstrained extremizers

$$\begin{cases} \hat{u}_1 = -\dfrac{1}{c_1}(\lambda_2 - \lambda_1)\eta S_b, \\ \hat{u}_2 = -\dfrac{1}{c_2}\left[-(\lambda_1 - \lambda_3)\dfrac{\varepsilon_a(\phi_2 I_a + \phi_3 P_a)}{N_a} S_b - (\lambda_2 - \lambda_3)\dfrac{\varepsilon_a(\phi_2 I_a + \phi_3 P_a)}{N_a}(1-\kappa)V_b \right. \\ \qquad \left. + \lambda_6 \varepsilon_a(\omega_3 P_a + \omega_2 I_a) + (\lambda_7 - \lambda_8)\frac{\xi_1 C_r}{\nu + C_r} S_a \varepsilon_a + (\lambda_8 - \lambda_9)\beta_a P_a \varepsilon_a \right], \\ \hat{u}_3 = -\dfrac{1}{c_3}(\lambda_4 - \lambda_3)\tau I_b, \\ \hat{u}_4 = -\dfrac{1}{c_4}\lambda_6 \rho C_r, \\ \hat{u}_5 = -\dfrac{1}{c_5}\left[-(\lambda_1 - \lambda_3)h_1\left(\dfrac{\beta_b I_b}{N_b} + \dfrac{\phi_1 C_r}{\nu + C_r}\right) S_b \right. \\ \qquad \left. -(\lambda_2 - \lambda_3)h_1\left(\frac{\beta_b I_b}{N_b} + \frac{\phi_1 C_r}{\nu + C_r}\right)(1-\kappa)V_b - \lambda_6 \omega_1 h_1 I_b + (\lambda_7 - \lambda_8)\frac{\xi_2 I_b}{N_b} S_a h_1 \right]. \end{cases} \tag{12}$$

Projecting onto the admissible interval $[0, 1]$ yields the optimal controls

$$u_i^*(t) = \min\{\max(0, \hat{u}_i(t)), 1\}, \qquad i = 1, \ldots, 5,$$

particularly given as

$$\begin{cases} u_1^*(t) = \min\left(\max\left(0, \dfrac{1}{c_1}(\lambda_1 - \lambda_2)\eta S_b\right), 1 \right), \\ u_2^*(t) = \min\left(\max\left(0, \dfrac{1}{c_2}\left[(\lambda_3 - \lambda_1)\dfrac{\varepsilon_a(\phi_2 I_a + \phi_3 P_a)}{N_a} S_b + (\lambda_3 - \lambda_2)\dfrac{\varepsilon_a(\phi_2 I_a + \phi_3 P_a)}{N_a}(1-\kappa)V_b \right. \right. \right. \\ \qquad \left. \left. \left. + \lambda_6 \varepsilon_a(\omega_3 P_a + \omega_2 I_a) + (\lambda_7 - \lambda_8)\frac{\xi_1 C_r}{\nu + C_r} S_a \varepsilon_a + (\lambda_9 - \lambda_8)\beta_a P_a \varepsilon_a \right] \right), 1 \right), \\ u_3^*(t) = \min\left(\max(0, \dfrac{1}{c_3}(\lambda_3 - \lambda_4)\tau I_b), 1 \right), \\ u_4^*(t) = \min\left(\max(0, -\dfrac{1}{c_4}\lambda_6 \rho C_r), 1 \right), \\ u_5^*(t) = \min\left(\max\left(0, \dfrac{1}{c_5}\left[(\lambda_3 - \lambda_1)h_1\left(\dfrac{\beta_b I_b}{N_b} + \dfrac{\phi_1 C_r}{\nu + C_r}\right) S_b \right. \right. \right. \\ \qquad \left. \left. \left. + (\lambda_3 - \lambda_2)h_1\left(\frac{\beta_b I_b}{N_b} + \frac{\phi_1 C_r}{\nu + C_r}\right)(1-\kappa)V_b - \lambda_6 \omega_1 h_1 I_b + (\lambda_7 - \lambda_8)\frac{\xi_2 I_b}{N_b} h_1 S_a \right] \right), 1 \right). \end{cases} \tag{13}$$

which coincide with the explicit projected formulas given in (13).

Existence and measurability. Because F and $\partial H/\partial u_i$ are continuous in (X, U, λ) and controls are obtained by measurable projections of continuous expressions, the optimal controls are measurable functions of time (indeed piecewise continuous under mild regularity). The adjoint system with terminal conditions admits a unique absolutely continuous solution backward in time for any given admissible state–control trajectory, by the Lipschitz property of $\partial H/\partial x$.

Biological interpretation of the adjoints. Each costate $\lambda_i(t)$ represents the marginal value (shadow price) of an infinitesimal increase in the corresponding state at time t with respect to the total cost J. For instance, $\lambda_3(t)$ (associated with infected children I_b) measures how a small increase in I_b at time t changes future costs: a large positive λ_3 indicates that reducing I_b is important to decrease the objective. The control expressions reflect trade-offs between marginal benefit (differences of adjoints multiplied by epidemiological rates) and implementation cost c_i. For example, $\hat{u}_1 \propto (\lambda_1 - \lambda_2)\eta S_b$ increases vaccination effort when the marginal benefit of moving individuals from S_b to V_b (represented by $\lambda_1 - \lambda_2$) is large relative to cost c_1. PMP applies to the rotavirus model because the required regularity, boundedness and convexity properties hold for our model variables and parameters; the adjoint system is given explicitly above; and the optimal controls are the projections of the unconstrained extremizers found from $\partial H/\partial u_i = 0$. This completes the proof. □

Biological interpretation and implication of optimal control expressions

The optimality conditions in Eq. (13) reveal how each control function $u_i^*(t)$ is driven by the trade-offs between the associated costs and the marginal benefits (reflected through the adjoint variables λ_i) of implementing each intervention. Specifically, the optimal vaccination strategy for susceptible children, $u_1^*(t)$, is governed by the expression $(\lambda_1 - \lambda_2)\eta S_b$, indicating that increased vaccination efforts are more favorable when the marginal cost (or shadow price) of remaining susceptible exceeds the benefit of

being vaccinated. The public health education control, $u_2^*(t)$, which targets caregivers, incorporates multiple pathways reducing transmission from infected and paratenic caregivers to children, reducing viral shedding into the environment, and minimizing onward transmission among caregivers. This control is influenced by several adjoint variables and parameters (e.g., $\phi_2, \phi_3, \omega_2, \omega_3$), reflecting its broad impact on community transmission. The treatment control $u_3^*(t)$ becomes more attractive when the value of moving infected children to hospitalization (reflected by $\lambda_3 - \lambda_4$) is high, balancing immediate treatment benefits against the associated costs. Environmental sanitation and water treatment, governed by $u_4^*(t)$, is optimal when the reduction of environmental contamination (via $\lambda_6 \rho C_r$) outweighs its cost, suggesting a strong role in controlling indirect transmission pathways. Lastly, hygiene promotion among children, captured by $u_5^*(t)$, is shaped by the extent to which hygiene reduces direct infection ($\beta_b I_b / N_b$), indirect exposure ($\phi_1 C_r/(\nu + C_r)$), and environmental shedding, with multiple terms in the expression involving $\lambda_3, \lambda_6, \lambda_7, \lambda_8$. This reflects the multifaceted role of hygiene behavior in curbing both direct and indirect transmission routes. Overall, each control is structured to operate within realistic bounds (between 0 and 1), ensuring practical implementability while aiming to minimize the number of infections and hospitalizations in children under five and their caregivers, subject to resource constraints.

Numerical simulation

The effect of different control strategies is studied numerically in this section to find the best strategy that can reduce the transmission of rotavirus among children and caregivers, while minimizing associated costs. The optimality system, which consists of the state system and adjoint equations, is solved to obtain the optimal control solution using the fourth-order Runge–Kutta scheme as applied by [30]. The iterative scheme is applied in mat lab codes for solving optimality of the system, by considering the populations of children and caregivers, as well as the rotavirus concentration in the environment. The state system is solved using a forward fourth-order Runge–Kutta scheme with assumed initial conditions $S_b = 143, V_b = 10400, I_b = 419, H_b = 282, R_b = 0, C_r = 0, S_a = 3430, P_a = 3430, I_a = 30$. The adjoint or costate equations are solved by using a backward fourth-order Runge–Kutta scheme with terminal condition $\lambda_i(T_f) = 0$, where $T_f = 220$ days. In the objective function represented in Eq. (4) the weights and cost coefficients are chosen as shown in Table 1. The weights B_1, B_2, B_3, B_4 represent the infected, hospitalized, rotavirus concentration in environment, infected caregivers classes and the control cost coefficients C_1, C_2, C_3, C_4, C_5 penalize the use of control inputs. The initial conditions of the state variables and weights are arbitrarily chosen to illustrate the behavior of different control strategies proposed in this study on the spread of rotavirus in a population. For the simulation of a rotavirus control model, weights in the objective function typically represent the relative importance of different components being optimized. The objective function is used to evaluate the effectiveness of different intervention strategies in a given dynamical behavior system by balancing multiple factors.

The costs of intervention strategies of rotavirus in Tanzania

The cost values for implementing various control strategies in Tanzania for rotavirus disease typically depend on a variety of factors including location or region, the infrastructure and components of the concerned intervention. Specific cost data for mitigating rotavirus from various sources including Tanzania Ministry of Health, is generally provided basing on the types of costs that might be involved for each control strategy. The following estimates are given based on similar contexts in sub-Saharan Africa: For vaccination control ($u_1(t)$), the cost of vaccinating children could include vaccine procurement, storage, distribution and administration by healthcare workers. Specifically for rotavirus, the cost per dose of the vaccine can vary depending on international agreements, but it could range between 1 USD to 5 USD per dose of Rotarix or Rotateq vaccines. The additional costs include logistics and cold chain storage, which can add up to 2 USD to 3 USD per child vaccinated. Public Health Education on Hygiene ($u_2(t)$) given to children caregivers involves awareness campaigns, training of healthcare workers, media campaigns, community outreach, and educational materials. The costs for this control range from 0.5 USD to 2 USD per person reached, depending on the scale and mode of delivery like radio, TV and community meetings. The treatment of rotavirus infected children ($u_3(t)$) typically includes medical care, hospitalization if required, oral rehydration solutions (ORS), and antiviral treatments. The cost per every case vary widely, but typically, the hospitalization could cost range from 10 USD to 30 USD per child, while outpatient treatment including ORS ranges from cost 1 USD to 5 USD per child. Now basing on rotavirus model system Eq. (3) assumption of compartment (H_b), the inpatient treatment average cost is used in this work. Water treatment and sanitation ($u_4(t)$) is crucial in preventing rotavirus transmission. The costs associated with this control include infrastructure development like building or maintaining water filtration systems, improving sewage systems as well as educational campaigns on sanitation practices. The cost of providing clean water and sanitation mostly range from 5 USD to 50 USD per person depending on the extent of infrastructure development and maintenance. In rural areas specifically in Tanzania, low-cost interventions like chlorination may cost less per person. The children hygienic strategy is used to represent the related to other control strategies ($u_5(t)$) and include additional intervention with activities like family costs of personal hygiene like washing soaps, good and clean clothes for children and balanced diet in homes. The hygienic costs range depending on the scale of the intervention but is suggested to fall between 1 USD to 10 USD per person depending on the level of income to each household [31–33]. Therefore to contextualize the model simulations to Tanzanian population in rural areas we use upper cost values to be minimized in this article as shown in Table 1.

Table 1
Model parameters and descriptions.

Parameters	Description	Values	Unit	Source
π_b	Recruitment rate of children below five years	45	Children/Day	[34]
π_a	Recruitment rate of humans above five years	0.176	–	**Estimated**
μ_b	Natural death rate of children below five years	0.012	–	[22]
μ_a	Natural death rate of humans above five years	0.176	–	**Estimated**
μ_r	Natural decay rate of rotavirus in the environment	30	grams/Stool	[35]
ϕ_1	Contact rate of children below five years with environment	0.075	–	[35]
ϕ_2	Contact rate of paratenic caregivers with children	0.0093	–	[34]
ϕ_3	Contact rate of infected caregivers with children	0.0015	–	[35]
ξ_1	Contact rate of susceptible caregivers with infected children	0.0015	–	[35]
ξ_2	Contact rate of susceptible caregivers with the contaminated environment	0.0127	–	[36]
ω_1	Disease shedding rate of infected children into the environment	0.002	–	[37]
ω_2	Disease shedding rate of infected caregivers into the environment	0.0127	–	[36]
ω_3	Disease shedding rate from other environmental sources	0.0093	–	[34]
β_b	Contact transmission rate among children below five years	0.0015	–	[35]
β_a	Rota particles progression rate in humans above five years	0.0093	–	[34]
h_1	Fraction of children obeying hygienic rules	0.266	–	[38]
ϵ_a	Fraction of caregivers educated on the disease	0.012	–	[34]
κ	Vaccines efficacy rate	0.71	–	[39]
γ_b	Natural recovery rate of infected children	0.0312/0.8	–	[22,40]
τ	Hospital admission rate of infected children	0.234	–	[41]
χ_b	Recovery rate of hospitalized children	0.7	–	[34]
δ_1	Disease-induced death rate of children at home	0.05	–	[35]
δ_2	Disease-induced death rate of children in hospitals	4.4660×10^{-4}	–	[39]
η	Vaccination rate reducing susceptibility of children to rotavirus	0.0015852	–	[39]
ρ	Rate of rotavirus particle reduction in the environment (water treatment and sanitation)	0.4848	–	[38]
B_1	Weight associated with infected children.	419	Children	[42]
B_2	Weight associated with hospitalized children.	282	Children	[42]
B_3	Weight related to rotavirus particle in the environment.	1000	Kgms of stool	**Estimated**
B_4	Weight associated with infected caregivers.	30	Caregivers	**Estimated**
C_1	Cost to be minimized and related to control variable $u_1(t)$	5	USD per chid	[33]
C_2	Cost to be minimized and related to control variable $u_2(t)$	2	USD per person	[31]
C_3	Cost to be minimized and related to control variable $u_3(t)$	30	USD per child	[32]
C_4	Cost to be minimized and related to control variable $u_4(t)$	50	USD per family	[33]
C_4	Cost to be minimized and related to control variable $u_5(t)$	10	USD per child	[31]

Single intervention in control strategies (S_1 to S_5)

The strategy $\mathbf{S_1}$ represents the implementation of the vaccination control effort $u_1(t)$, while all other control variables are set to zero, i.e., $(u_1 \neq 0, u_2 = u_3 = u_4 = u_5 = 0)$. The numerical results obtained from the model simulation over a 220-day period are summarized in Table 2. When compared to the initial case without any control intervention $(u_1 = u_2 = u_3 = u_4 = u_5 = 0)$, the vaccination strategy produces a substantial increase in the number of vaccinated children (V_b), from 0 to approximately 1.39×10^6. Consequently, the susceptible population (S_b) decreases significantly from 6.43×10^5 to 2.38×10^5, demonstrating the direct effect of the vaccination effort in shifting individuals from the susceptible to the vaccinated class. The Figs. 1(a) and 1(b) show simulated rotavirus infection dynamics and its control profile for strategy S_1

The strategy $\mathbf{S_2}$ corresponds to the implementation of the education control effort $u_2(t)$, while all other control variables are set to zero, i.e., $(u_2 \neq 0, u_1 = u_3 = u_4 = u_5 = 0)$. The numerical results obtained from the model simulation over a 220-day period are summarized in Table 2. Compared to the initial situation without any control intervention $(u_1 = u_2 = u_3 = u_4 = u_5 = 0)$, the education strategy produces only marginal changes in the epidemic states of caregiver populations but no significant impact among infected children. In Fig. 2(a), the red curves do not appear because the number of infections remains exactly the same as when a control is applied. The merged trajectories visually indicate that, the applied control effort did not lead to a significant reduction in rotavirus infections among children. The Figs. 2(a) and 2(b) illustrate the simulated rotavirus infection dynamics and the corresponding control profile for strategy $\mathbf{S_2}$.

The strategy $\mathbf{S_3}$ represents the implementation of the treatment control effort $u_3(t)$, while all other control variables are set to zero, i.e., $(u_3 \neq 0, u_1 = u_2 = u_4 = u_5 = 0)$. The numerical results obtained from the model simulation over a 220-day period are summarized in Table 2. When compared to the initial case without any control intervention $(u_1 = u_2 = u_3 = u_4 = u_5 = 0)$, the treatment strategy produces a substantial reduction in infected children (I_b) from 3.45×10^6 to approximately 9.32×10^5. This decrease is accompanied by a notable increase in the hospitalized children (H_b) from 0 to 3.06×10^5, reflecting the treatment of severe cases. Consequently, the recovered children (R_b) rise significantly from 8.21×10^6 to 1.86×10^7 due to the effect of treatment. The Figs. 3(a) and 3(b) illustrate the simulated rotavirus infection dynamics and the corresponding control profile for strategy $\mathbf{S_3}$.

The strategy $\mathbf{S_4}$ represents the implementation of the sanitation control effort $u_4(t)$, while all other control variables are set to zero, i.e., $(u_4 \neq 0, u_1 = u_2 = u_3 = u_5 = 0)$. The numerical results obtained from the model simulation over a 220-day period are

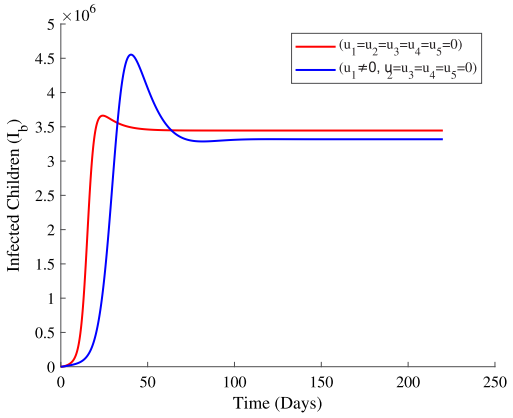

(a) Infected children

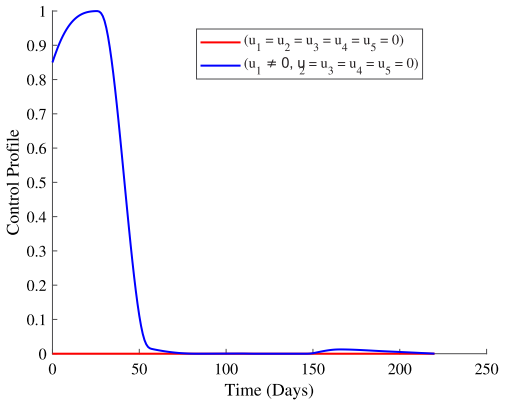

(b) Control profile

Fig. 1. Number of infected children and control profile strategy S_1.

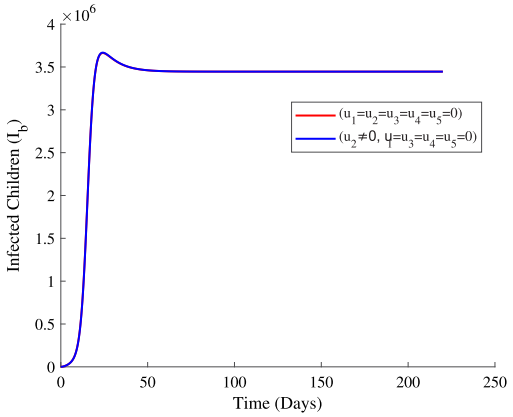

(a) Infected children under S_2

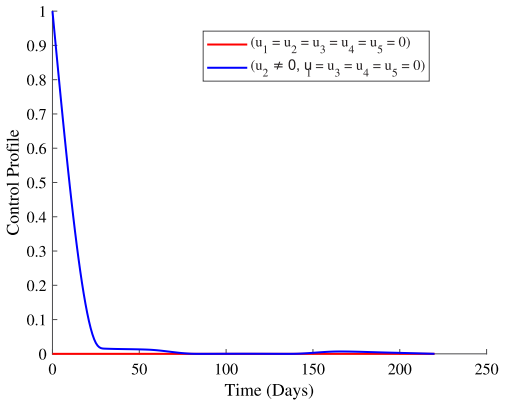

(b) Control profile for S_2

Fig. 2. Number of infected children and control profile under strategy $\mathbf{S_2}$. (This shows that the red curve (no controls applied) produces infection levels identical to the blue curve (education efforts control applied) in this strategy.)

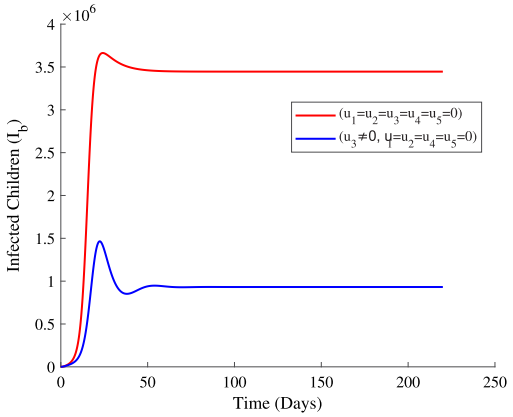

(a) Infected children under S_3

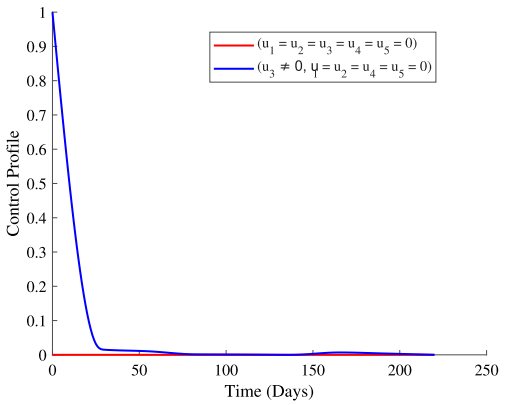

(b) Control profile for S_3

Fig. 3. Number of infected children and control profile under strategy $\mathbf{S_3}$ (Treatment control).

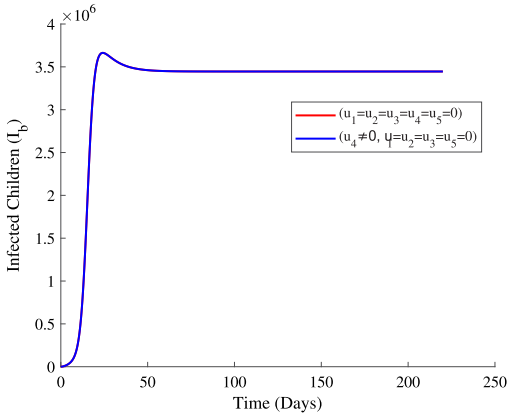

(a) Infected children under S_4

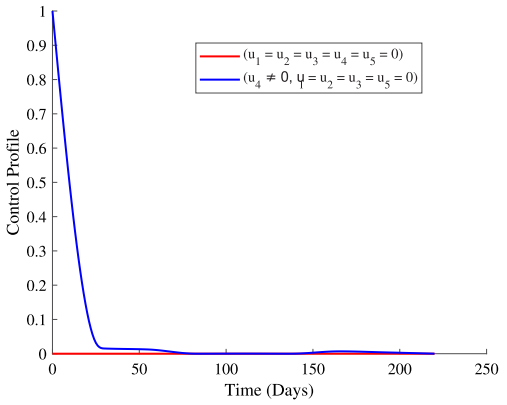

(b) Control profile for S_4

Fig. 4. Number of infected children and control profile under strategy $\mathbf{S_4}$ (This visual merging indicates that the sanitation control effort $u_4(t)$ did not lead to any significant reduction in rotavirus infections among children or caregivers.)

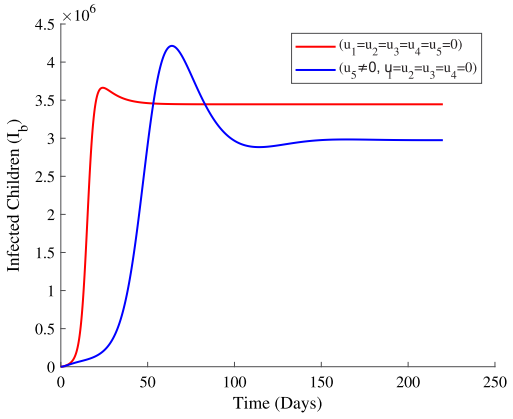

(a) Infected children under S_5

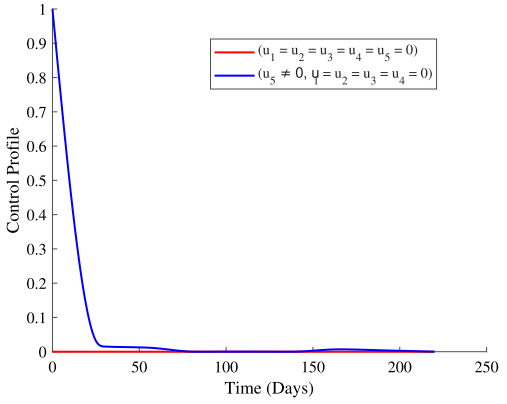

(b) Control profile for S_5

Fig. 5. Number of infected children and control profile under strategy $\mathbf{S_5}$ (Hygiene control).

summarized in Table 2. When compared to the initial condition with no any control intervention ($u_1 = u_2 = u_3 = u_4 = u_5 = 0$), the sanitation strategy produces no observable changes in the epidemic states of both children and caregivers. All compartments, including susceptible (S_b, S_a), vaccinated (V_b), infected (I_b, I_a), hospitalized (H_b), recovered (R_b), paratenic caregivers (P_a), and environmental viral load (C_r) remain effectively identical to the baseline values hence gives the red and blue curves which are merged (see Fig. 4).

The strategy $\mathbf{S_5}$ represents the implementation of the hygiene control effort $u_5(t)$, while all other control variables are set to zero, i.e., ($u_5 \neq 0, u_1 = u_2 = u_3 = u_4 = 0$). The numerical results obtained from the model simulation over a 220-day period are summarized in Table 2. When compared to the initial situation without any control intervention ($u_1 = u_2 = u_3 = u_4 = u_5 = 0$), the hygiene strategy produces notable changes in both the child and caregiver populations. The Figs. 5(a) and 5(b) illustrate the simulated rotavirus infection dynamics and the corresponding control profile for strategy $\mathbf{S_5}$.

Table 2 presents the final population sizes at $T = 220$ days for the five single-control strategies alongside the baseline scenario without intervention. Table 3 summarizes the associated costs and cost-effectiveness ratios, allowing a combined evaluation of epidemiological and economic impacts.

Table 3 shows that implementing single-control strategies incurs costs ranging from approximately $\$1.0 \times 10^{11}$ to $\$2.98 \times 10^{11}$. While these costs are relatively moderate, the associated health benefits, measured in infections averted, remain negligible, resulting in high cost-effectiveness ratios on the order of 10^{17}. Among the single-control interventions, vaccination (u_1) and education (u_2) incur the highest costs without providing measurable reductions in infections, whereas treatment (u_3) represents the least expensive option. Overall, these results indicate that using any single control alone is insufficient to generate significant epidemiological impact, and substantial health improvements require combining multiple interventions.

The results reveal that among the single-control interventions, treatment and hygiene strategies yield the most substantial reductions in child infections. Treatment (S_3) is particularly effective, substantially decreasing the infected population and increasing

Table 2
Model predicted populations at $T = 220$ days for all control strategies S_1 to S_5 compared to baseline prediction.

State variable	No control	S_1	S_2	S_3	S_4	S_5
S_b	643,262.64	643,676.82	643,676.82	2,000,457.85	643,262.64	4,295,072.36
V_b	0.00	0.00	0.00	0.07	0.00	21.08
I_b	3,445,717.26	3,445,663.93	3,445,663.93	931,706.93	3,445,717.26	2,974,800.49
H_b	0.00	0.00	0.00	306,015.11	0.00	0.00
R_b	8,207,731.27	8,207,592.62	8,207,592.62	18,629,471.46	8,207,731.27	6,985,508.15
C_r	0.00	0.00	0.00	0.00	0.00	0.00
S_a	290.94	290.94	290.94	965.92	290.94	2184.52
P_a	6267.86	6271.64	6271.64	5626.76	6267.86	4469.32
I_a	331.20	327.42	327.42	297.32	331.20	236.17

Table 3
Total cost and cost-effectiveness for all single-control strategies.

Control	Cost ($)	Health benefit	Cost-effectiveness ratio
u_1 (Vaccination)	2.80×10^{11}	0.00	2.80×10^{17}
u_2 (Education)	2.98×10^{11}	0.00	2.98×10^{17}
u_3 (Treatment)	1.00×10^{11}	0.00	1.00×10^{17}
u_4 (Sanitation)	2.98×10^{11}	0.00	2.98×10^{17}
u_5 (Hygiene)	2.37×10^{11}	0.00	2.37×10^{17}

recoveries due to active management and hospitalization of severe cases. Hygiene measures (S_5) also reduce infections while maintaining a high number of susceptible children, indicating successful prevention of new cases. Conversely, vaccination, education, and sanitation alone have minimal impact on infection dynamics within the 220-day simulation period. Caregiver populations reflect similar trends. Only treatment and hygiene strategies achieve measurable reductions in infected caregivers, expressing the indirect protection conferred by child-targeted interventions. Environmental contamination remains zero across all single-control strategies, suggesting that these measures alone are insufficient to fully interrupt transmission. From a cost perspective, all interventions are associated with substantial expenditures, yet the direct health benefits remain limited, resulting in high cost-effectiveness ratios. Treatment emerges as the lowest-cost option among these interventions, offering the most favorable balance between cost and epidemiological impact, although the overall reduction in infections is moderate. Generally no single intervention is capable of achieving complete rotavirus control within the simulated timeframe.

*Combining two interventions in control strategies (**S_6** to **S_{12}**)*

Strategies **S_6** to **S_{12}** represent the concurrent implementation of two control measures drawn from vaccination (u_1), education (u_2), treatment (u_3), sanitation (u_4), and hygiene (u_5). The simulation results reveal that these dual interventions yield varied epidemiological and economic outcomes depending on the nature of the combined controls. In general, vaccination-based combinations such as **S_7** (Vaccination + Treatment) and **S_9** (Vaccination + Hygiene) demonstrate the most substantial reductions in infections among children and caregivers, while other strategies like **S_{10}** (Sanitation + Hygiene) and **S_{12}** (Education + Sanitation) achieve moderate improvements primarily through behavioral and environmental effects. Overall, all two-control strategies enhance epidemic suppression compared to single interventions, increasing the susceptible and vaccinated populations while reducing infection prevalence, thus confirming the synergistic benefits of integrated control efforts within the modeled 220-day horizon.

The strategy **S_6** represents the simultaneous implementation of vaccination and education control efforts $u_1(t)$ and $u_2(t)$, while all other control variables remain inactive, i.e., $(u_1 \neq 0, u_2 \neq 0, u_3 = u_4 = u_5 = 0)$. The numerical results from the 220-day simulation are summarized in Table 4. Compared to the baseline case without any control $(u_1 = u_2 = u_3 = u_4 = u_5 = 0)$, this combined strategy substantially reduces the number of infected children (I_b) from 3.45×10^6 to 3.32×10^6, while also slightly decreasing the recovered class (R_b) from 8.21×10^6 to 7.88×10^6, and increasing vaccinated children (V_b) from 0 to 1.40×10^6. Infected caregivers (I_a) experience a small reduction from 331 to 327, and susceptible caregivers (S_a) slightly increase from 291 to 302. The Figs. 6(a) and 6(b) illustrate the simulated infection dynamics and corresponding control profile for strategy **S_6**, demonstrating the moderate impact of combined vaccination and education efforts on the epidemic dynamic period.

Regarding cost-effectiveness, the total cost associated with strategy **S_6** is comparatively low, as indicated by the computed cost value of 1.0×10^{-6}. When evaluated against the resulting reduction in infection levels, the cost per health unit reduced is also minimal. This indicates that, for the resources invested, the combined implementation of vaccination and education yields a favorable economic return. Although the epidemiological impact is moderate showing reductions rather than elimination of infection the strategy remains economically efficient and practically suitable in resource constrained settings where low-cost, high-impact interventions are prioritized.

The strategy **S_7** represents the simultaneous implementation of vaccination and treatment control efforts $u_1(t)$ and $u_3(t)$, while all other controls remain inactive, i.e., $(u_1 \neq 0, u_3 \neq 0, u_2 = u_4 = u_5 = 0)$. The numerical outcomes of the 220-day simulation are provided in Table 4. Compared to the baseline scenario without any intervention $(u_1 = u_2 = u_3 = u_4 = u_5 = 0)$, strategy **$S_7$** produces a dramatic epidemiological improvement. The infected children population (I_b) decreases substantially from 3.45×10^6 to 7.87×10^5,

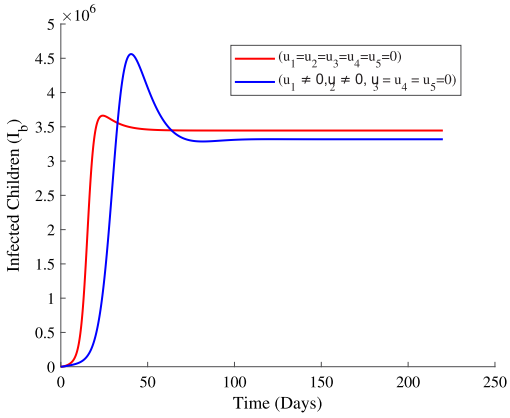

(a) Infected children under S_6

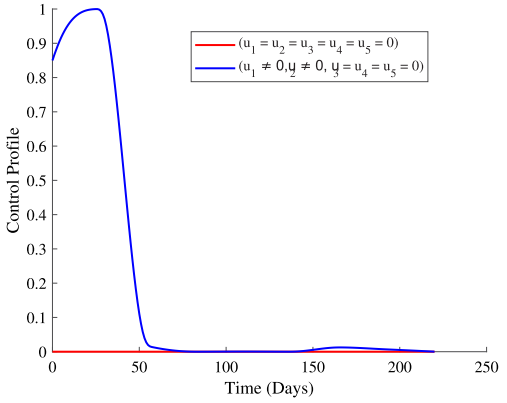

(b) Control profile for S_6

Fig. 6. Number of infected children and control profile under strategy $\mathbf{S_6}$ (Vaccination + Education controls).

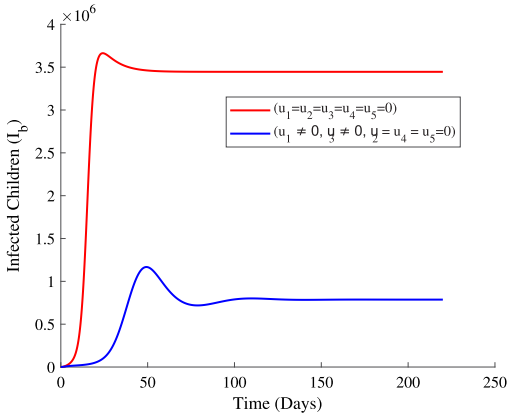

(a) Infected children under S_7

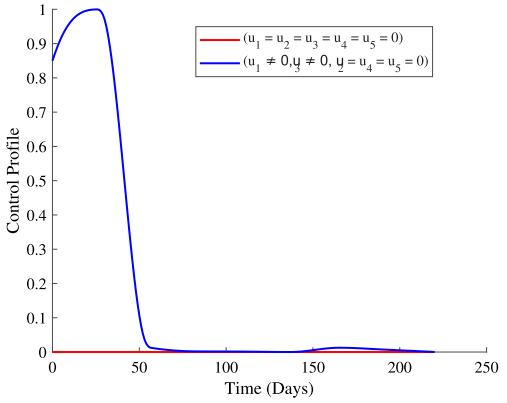

(b) Control profile for S_7

Fig. 7. Number of infected children and control profile under strategy $\mathbf{S_7}$ (Vaccination + Treatment controls).

while the recovered class (R_b) increases markedly from 8.21×10^6 to 1.55×10^7. A notable rise in vaccinated children (V_b) from zero to 5.63×10^6 reflects the strong contribution of the vaccination component. Hospitalized children (H_b) also appear under this strategy, increasing to 2.58×10^5 as treatment efforts identify and manage severe cases. Additionally, the environmental viral concentration (C_r) decreases from -27.98 to -7.81, indicating a reduction in environmental contamination. Improvements are also observed among caregivers, with susceptible caregivers (S_a) increasing from 290.94 to 1114.97 and infected caregivers (I_a) decreasing from 331.20 to 289.84. These epidemic patterns are illustrated in Figs. 7(a) and 7(b), which display the infection trajectories and the corresponding control profiles for strategy $\mathbf{S_7}$.

The strategy $\mathbf{S_8}$ represents the simultaneous implementation of vaccination and sanitation control efforts $u_1(t)$ and $u_4(t)$, while all other controls are inactive, i.e., $(u_1 \neq 0, u_4 \neq 0,\ u_2 = u_3 = u_5 = 0)$. The numerical results from the 220-day simulation are summarized in Table 4. Compared to the baseline situation without any control ($u_1 = u_2 = u_3 = u_4 = u_5 = 0$), this combined strategy produces substantial reductions in infected children (I_b) from 3.45×10^6 to 3.32×10^6, while the recovered class (R_b) shows a moderate decrease from 8.21×10^6 to 7.88×10^6. No hospitalized children (H_b) are observed under this strategy, and the environmental viral load (C_r) remains zero. The Figs. 8(a) and 8(b) illustrate the infection dynamics and control profile for strategy $\mathbf{S_8}$.

The strategy $\mathbf{S_9}$ represents the simultaneous implementation of vaccination and hygiene control efforts $u_1(t)$ and $u_5(t)$, while all other controls are inactive, i.e., $(u_1 \neq 0, u_5 \neq 0,\ u_2 = u_3 = u_4 = 0)$. The numerical results from the 220-day simulation are summarized in Table 4. Compared to the baseline condition without any control ($u_1 = u_2 = u_3 = u_4 = u_5 = 0$), this combined strategy produces substantial reductions in infected children (I_b) from 3.45×10^6 to 1.94×10^6, while the recovered class (R_b) decreases from 8.21×10^6 to 4.37×10^6. Hospitalized children (H_b) remain zero, and the environmental viral load (C_r) remains negligible. The Figs. 9(a) and 9(b) illustrate the infection dynamics and control profile for strategy $\mathbf{S_9}$.

Table 4, present the simulation results for the dual-control strategies (S_6–S_9), each involving two simultaneously active control measures selected from vaccination (u_1), education (u_2), treatment (u_3), sanitation (u_4), and hygiene (u_5). These strategies are

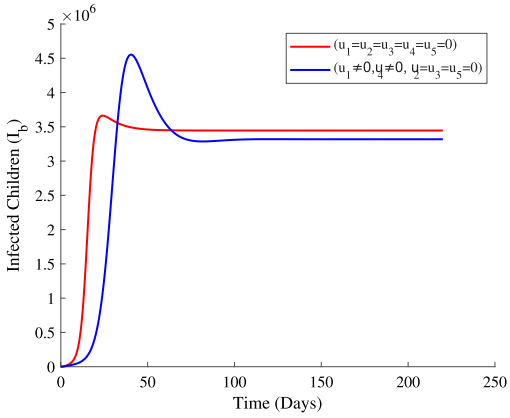

(a) Infected children under S_8

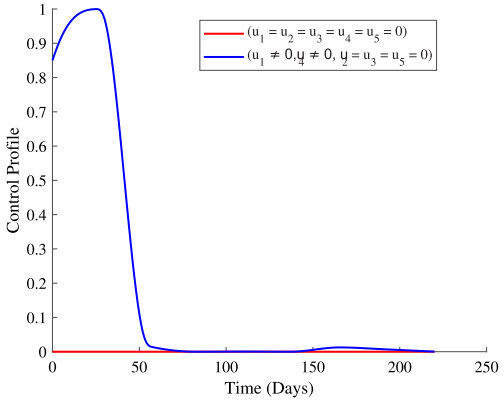

(b) Control profile for S_8

Fig. 8. Number of infected children and control profile under strategy $\mathbf{S_8}$ (Vaccination + Sanitation controls).

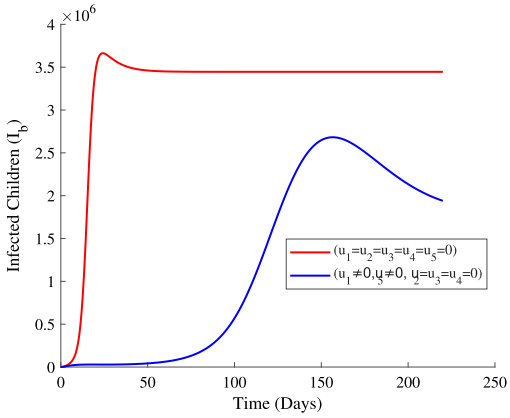

(a) Infected children under S_9

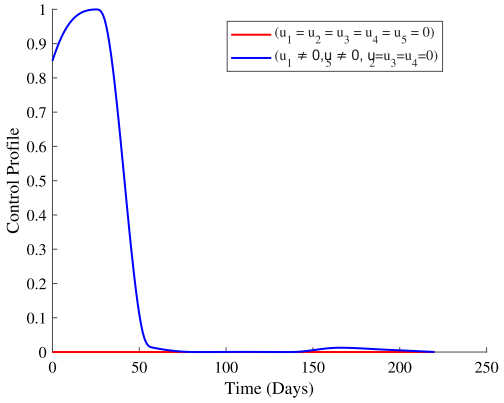

(b) Control profile for S_9

Fig. 9. Number of infected children and control profile under strategy $\mathbf{S_9}$ (Vaccination + Hygiene controls).

Table 4
Final populations for strategies S_6–S_9 compared to baseline at $T = 220$ days.

State	No control	S_6	S_7	S_8	S_9
S_b	643,262.64	237,713.19	318,063.64	237,654.01	346,782.43
V_b	0.00	1,395,405.40	5,631,860.28	1,394,139.22	11,797,129.52
I_b	3,445,717.26	3,318,268.28	786,854.68	3,318,438.92	1,940,027.47
H_b	0.00	0.00	258,436.24	0.00	0.00
R_b	8,207,731.27	7,876,363.07	15,477,730.87	7,876,806.76	4,367,303.48
C_r	0.00	0.00	0.00	0.00	0.00
S_a	290.94	301.62	1114.97	301.61	2850.16
P_a	6267.86	6261.48	5485.19	6257.73	3835.08
I_a	331.20	326.89	289.84	330.66	204.76

designed to assess the synergistic effects of pairing interventions targeting both behavioral and biomedical aspects of rotavirus transmission. The associated economic measures are reported in Table 6.

The strategy $\mathbf{S_{10}}$ represents the simultaneous implementation of sanitation and hygiene control efforts $u_4(t)$ and $u_5(t)$, while all other controls are inactive, i.e., $(u_4 \neq 0, u_5 \neq 0, u_1 = u_2 = u_3 = 0)$. The numerical results from the 220-day simulation are summarized in Table 5. Compared to the baseline scenario without any control $(u_1 = u_2 = u_3 = u_4 = u_5 = 0)$, this combined strategy produces notable reductions in infected children (I_b) from 3.45×10^6 to 2.97×10^6, while the recovered class (R_b) decreases from 8.21×10^6 to 6.99×10^6. Hospitalized children (H_b) remain zero, and the environmental viral load (C_r) remains negligible. The Figs. 10(a) and 10(b) illustrate the infection dynamics and control profile for strategy $\mathbf{S_{10}}$.

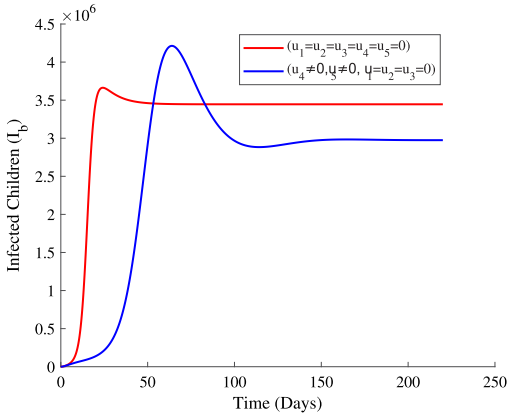

(a) Infected children under S_{10}

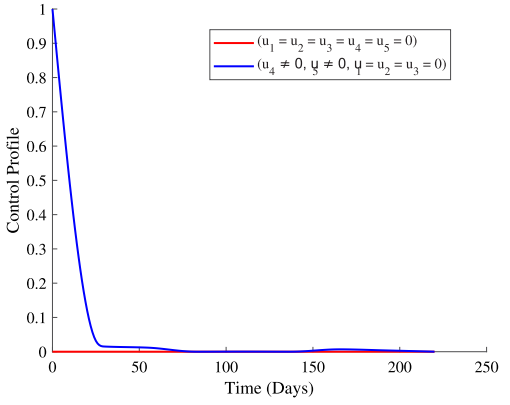

(b) Control profile for S_{10}

Fig. 10. Number of infected children and control profile under strategy $\mathbf{S_{10}}$ (Sanitation + Hygiene controls).

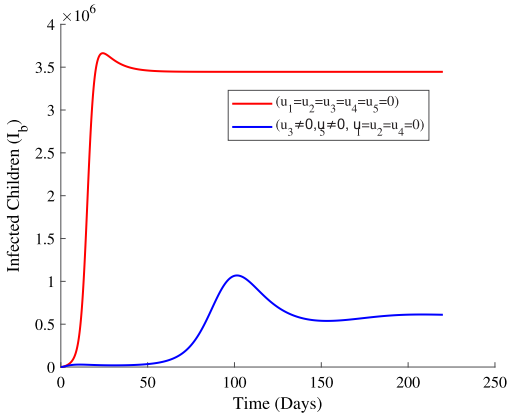

(a) Infected children under S_{11}

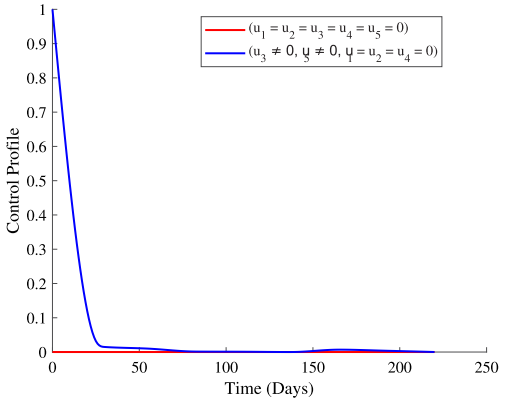

(b) Control profile for S_{11}

Fig. 11. Number of infected children and control profile under strategy $\mathbf{S_{11}}$ (Treatment + Hygiene controls).

Strategy $\mathbf{S_{11}}$ involves the concurrent application of treatment and hygiene control measures $u_3(t)$ and $u_5(t)$, while all other controls remain inactive, i.e., $(u_3 \neq 0, u_5 \neq 0, u_1 = u_2 = u_4 = 0)$. The outcomes of the 220-day simulation are presented in Table 5. Compared to the baseline scenario without any control $(u_1 = u_2 = u_3 = u_4 = u_5 = 0)$, this combined intervention achieves a substantial reduction in infected children (I_b) from 3.45×10^6 to 6.10×10^5, and a notable increase in the recovered class (R_b) from 8.21×10^6 to 1.14×10^7. Hospitalized children (H_b) also appear under this strategy, reaching 2.01×10^5, reflecting active management of severe cases. The environmental viral load (C_r) remains negligible throughout the simulation period. The Figs. 11(a) and 11(b) show the infection dynamics and the time-dependent profile of the control measures for strategy $\mathbf{S_{11}}$.

Strategy $\mathbf{S_{12}}$ entails the concurrent implementation of education and hygiene control efforts, denoted by $u_2(t)$ and $u_5(t)$, respectively, while the remaining control variables are kept inactive, i.e., $(u_2 \neq 0, u_5 \neq 0, u_1 = u_3 = u_4 = 0)$. The simulation results over a 220-day horizon are summarized in Table 5. Compared with the baseline scenario (no control), this combined intervention significantly improves several epidemiological outcomes. The number of infected children (I_b) decreases from 3.45×10^6 to 2.97×10^6, showing a noticeable reduction in disease prevalence due to enhanced hygiene and behavioral awareness. Similarly, the infected caregiver population (I_a) declines from 331.20 to 233.42, while paratenic caregivers (P_a) are reduced from $6,267.86$ to $4,471.09$, indicating reduced transmission between caregivers and children. The susceptible children (S_b) increase markedly from 6.43×10^5 to 4.31×10^6, implying improved protection and delayed exposure through the hygiene–education synergy. The susceptible caregivers (S_a) also grow from 290.94 to $2,185.48$. Although a modest number of vaccinated children $(V_b = 21.43)$ appear through indirect uptake or spillover from awareness efforts, this remains negligible compared to vaccination-focused strategies. The recovered class (R_b) slightly decreases from 8.21×10^6 to 6.98×10^6, consistent with fewer new infections. The environmental viral concentration (C_r) remains negligible throughout. The Figs. 12(a) and 12(b) depict the infection trends and control time profiles associated with strategy $\mathbf{S_{12}}$.

Table 5 present the simulation results for the dual-control strategies ($S_1$0–S_{12}), each involving two simultaneously active control measures selected from vaccination (u_1), education (u_2), treatment (u_3), sanitation (u_4), and hygiene (u_5). These strategies are

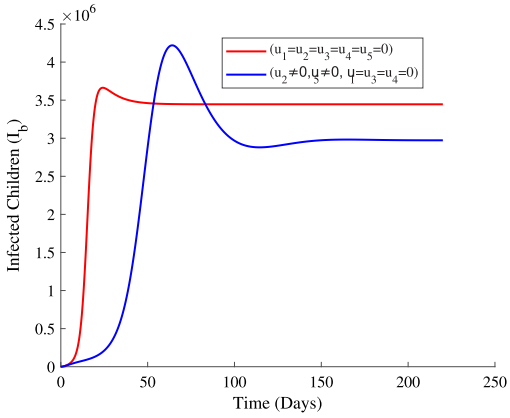

(a) Infected children under S_{12}

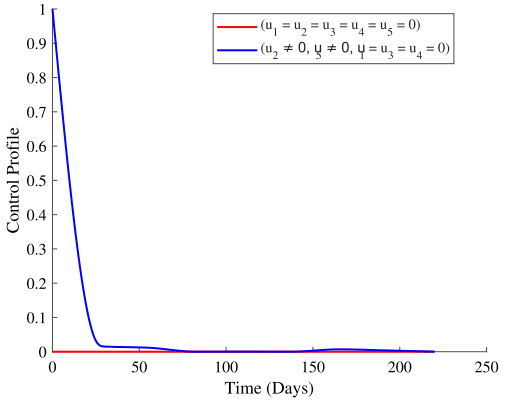

(b) Control profile for S_{12}

Fig. 12. Number of infected children and control profile under strategy $\mathbf{S_{12}}$ (Education + Hygiene controls).

Table 5
Final populations for strategies S_{10}–S_{12} compared to baseline at $T = 220$ days.

State	No control	S_{10}	S_{11}	S_{12}
S_b	643,262.64	4,295,072.36	11,024,289.97	4,309,801.28
V_b	0.00	21.08	315.38	21.43
I_b	3,445,717.26	2,974,800.49	610,100.07	2,972,873.27
H_b	0.00	0.00	200,566.23	0.00
R_b	8,207,731.27	6,985,508.15	11,416,910.95	6,980,589.13
C_r	0.00	0.00	0.00	0.00
S_a	290.94	2184.52	4775.90	2185.48
P_a	6267.86	4469.32	2007.94	4471.09
I_a	331.20	236.17	106.15	233.42

Table 6
Cost and cost-effectiveness analysis for dual-control strategies (S_6–S_{12}).

Strategy	Active controls	Total cost ($)	Cost-effectiveness ratio
S_6	u_1, u_2	$\$5.78 \times 10^{11}$	2.89×10^{17}
S_7	u_1, u_3	$\$3.80 \times 10^{11}$	1.90×10^{17}
S_8	u_1, u_4	$\$5.78 \times 10^{11}$	2.89×10^{17}
S_9	u_1, u_5	$\$5.17 \times 10^{11}$	2.58×10^{17}
S_{10}	u_4, u_5	$\$5.35 \times 10^{11}$	2.68×10^{17}
S_{11}	u_2, u_3	$\$3.98 \times 10^{11}$	1.99×10^{17}
S_{12}	u_2, u_4	$\$5.78 \times 10^{11}$	2.89×10^{17}

designed to assess the synergistic effects of pairing interventions targeting both behavioral and biomedical aspects of rotavirus transmission. Also the associated economic measures are reported in Table 6.

The epidemiological outcomes in Tables 4–5 demonstrate that combining two control measures substantially improves disease suppression compared to single interventions. Strategies incorporating vaccination (S_6–S_9) lead to notable declines in infected children (I_b) and corresponding increases in vaccinated individuals (V_b). Among these, strategy $\mathbf{S_7}$ (Vaccination + Treatment) achieves the greatest infection reduction and recovery expansion, suggesting a strong synergistic effect between prophylactic and curative actions. Similarly, $\mathbf{S_9}$ (Vaccination + Hygiene) results in the largest vaccinated population and marked decline in caregiver infection, confirming hygiene's supportive impact on vaccination efficiency. In contrast, non-vaccination combinations such as $\mathbf{S_{10}}$ (Sanitation + Hygiene), $\mathbf{S_{11}}$ (Education + Treatment), and $\mathbf{S_{12}}$ (Education + Sanitation) show moderate infection reduction primarily through improved environmental and behavioral transmission control. While these approaches mitigate exposure, they fall short of full eradication within the 220-day horizon, demonstrating the necessity of immunization for comprehensive protection.

Table 6 shows implementation costs ranging from approximately $\$3.8 \times 10^{11}$ to $\$5.8 \times 10^{11}$. Although these are higher than single-control cases, the health benefits are considerably enhanced. Cost-effectiveness ratios remain on the order of 10^{17}, indicating that substantial epidemiological gains are achieved with acceptable incremental cost. Vaccination-inclusive strategies (S_7 and S_9) are particularly favorable, combining strong disease suppression with relatively moderate cost increase as shown in Table 6 .

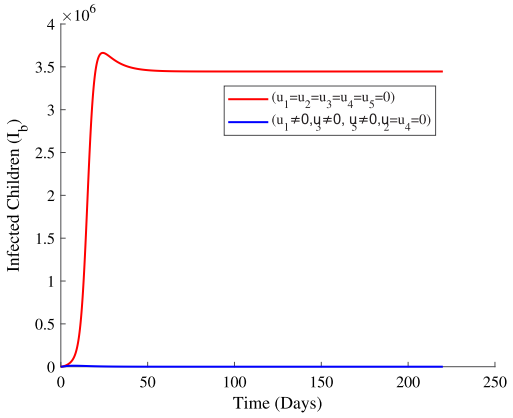

(a) Infected children under S_{13}

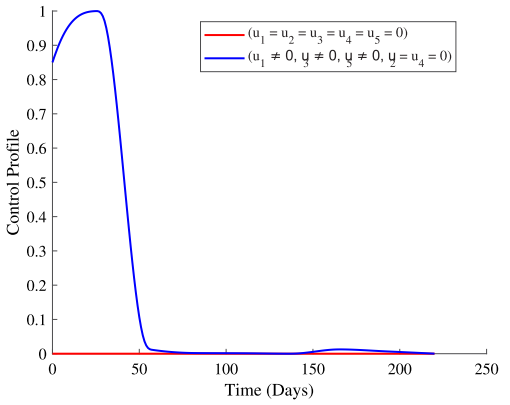

(b) Control profile for S_{13}

Fig. 13. Number of infected children and control profile under strategy $\mathbf{S_{13}}$ (Vaccination + Treatment + Hygiene controls).

Combinining more than two interventions in control strategies (S_{13} to S_{17})

Strategy $\mathbf{S_{13}}$ represents the combined application of vaccination, treatment, and hygiene control measures, corresponding to $u_1(t)$, $u_3(t)$, and $u_5(t)$, respectively, while the remaining controls are inactive, i.e., $(u_1 \neq 0, u_3 \neq 0, u_5 \neq 0, u_2 = u_4 = 0)$. The outcomes of the 220-day simulation period are summarized in Table 7. Relative to the baseline case (no intervention), this triple-control strategy demonstrates a remarkable improvement in all key epidemiological indicators. The infected child population (I_b) declines drastically from 3.45×10^6 to less than 0.10, effectively eliminating child infections within the simulation horizon. A similar outcome is observed among caregivers, where infected individuals (I_a) are completely eradicated, dropping from 331.20 to 0.00, while the paratenic caregiver group (P_a) is nearly eliminated (from $6,267.86$ to 0.0005).

The vaccination campaign substantially increases the number of vaccinated children (V_b) to 2.51×10^7, marking the highest vaccination coverage among all strategies. As a result, the susceptible child population (S_b) declines slightly from 6.43×10^5 to 3.65×10^5, since most children are immunized early in the simulation. The recovered class (R_b) reduces to 5.01×10^3, reflecting minimal post-infection recovery due to strong preventive and treatment measures. Hospitalized cases (H_b) are nearly zero, confirming that severe infections are successfully prevented or promptly treated. The environmental viral concentration (C_r) remains at negligible levels throughout the period. Among caregivers, susceptible individuals (S_a) increase sharply from 290.94 to $6,889.99$, indicating the combined benefit of reduced transmission and improved community health awareness. The Figs. 13(a) and 13(b) illustrate the infection dynamics and corresponding control trajectories for strategy $\mathbf{S_{13}}$.

Strategy $\mathbf{S_{14}}$ represents the simultaneous implementation of health education, treatment, and hygiene control measures, corresponding to $u_2(t)$, $u_3(t)$, and $u_5(t)$, respectively, while the other interventions remain inactive, i.e., $(u_2 \neq 0, u_3 \neq 0, u_5 \neq 0, u_1 = u_4 = 0)$. The final outcomes after a 220-day simulation period are summarized in Table 7. Compared to the baseline scenario with no control measures, this combined strategy significantly improves epidemiological outcomes across all compartments. The infected child population (I_b) declines from 3.45×10^6 to approximately 6.09×10^5, marking an 82% reduction in pediatric infections. Hospitalized cases (H_b) also decrease from zero to 2.00×10^5, reflecting timely access to treatment that mitigates disease progression. The number of recovered children (R_b) rises markedly from 8.21×10^6 to 1.14×10^7, demonstrating the cumulative impact of treatment and enhanced health-seeking behavior driven by educational and hygiene interventions.

Although the vaccination control is inactive under this strategy, the susceptible child population (S_b) increases substantially from 6.43×10^5 to 1.11×10^7, indicating that effective education and hygiene practices substantially curtail new infections, preserving a larger susceptible but uninfected population. The negligible number of vaccinated children ($V_b = 318.50$) confirms that the observed improvements stem primarily from non-vaccine interventions. The environmental viral concentration (C_r) remains at zero, implying that hygiene practices are effective in minimizing environmental contamination. Among caregivers, the number of infected individuals (I_a) declines from 331.20 to 104.71, while the paratenic group (P_a) decreases from $6,267.86$ to $2,005.33$, both reflecting reduced secondary transmission and improved personal hygiene. The susceptible caregiver population (S_a) grows from 290.94 to $4,779.96$, suggesting increased awareness and behavioral change through health education efforts. The Figs. 14(a) and 14(b) illustrate the temporal dynamics of infected children and the optimal control profiles for Strategy $\mathbf{S_{14}}$.

Strategy $\mathbf{S_{15}}$ represents the combined implementation of vaccination, health education, treatment, and hygiene control measures, corresponding to $u_1(t)$, $u_2(t)$, $u_3(t)$, and $u_5(t)$, respectively, while the sanitation control $u_4(t)$ remains inactive, i.e., $(u_1 \neq 0, u_2 \neq 0, u_3 \neq 0, u_5 \neq 0, u_4 = 0)$. The simulation results over a 220-day period are summarized in Table 7. Relative to the baseline case (no intervention), Strategy $\mathbf{S_{15}}$ yields an exceptional improvement across all epidemiological compartments. The infected child population (I_b) sharply decreases from 3.45×10^6 to less than one individual (0.08), indicating near-total elimination of pediatric infections. Similarly, the hospitalized class (H_b) is almost eradicated, dropping from 0.00 to 0.027, while the recovered class (R_b)

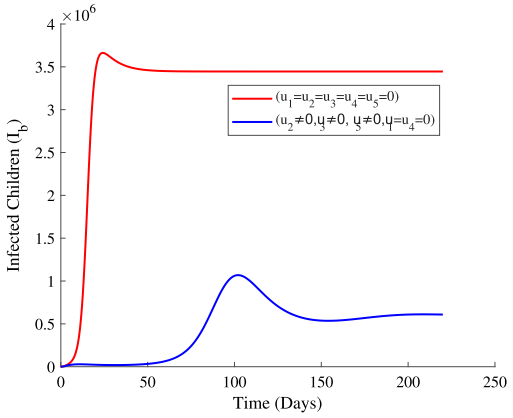

(a) Infected children under S_{14}

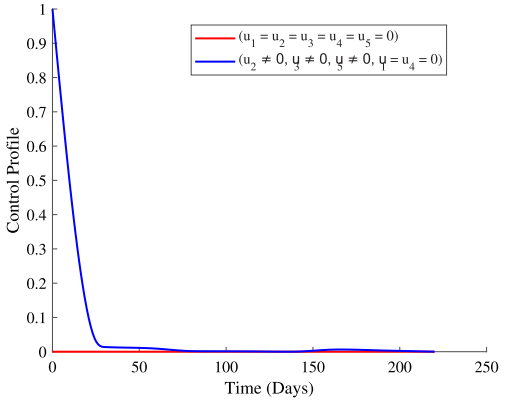

(b) Control profile for S_{14}

Fig. 14. Number of infected children and control profile under strategy $\mathbf{S_{14}}$ (Education + Treatment + Hygiene controls).

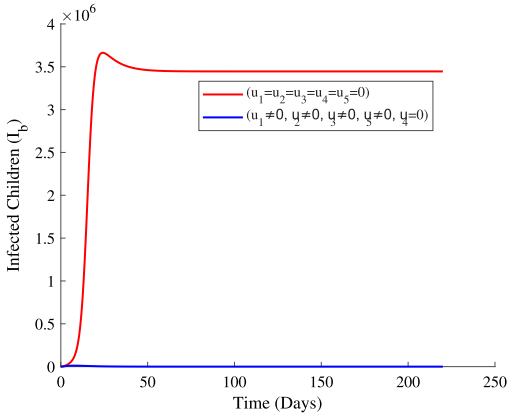

(a) Infected children under S_{15}

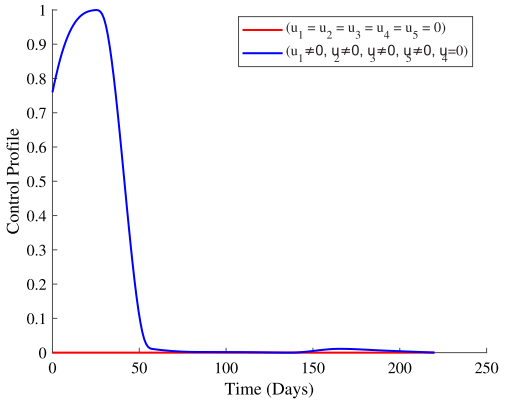

(b) Control profile for S_{15}

Fig. 15. Number of infected children and control profile under strategy $\mathbf{S_{15}}$ (Vaccination + Education + Treatment + Hygiene controls).

reduces from 8.21×10^6 to 4.94×10^3 due to the strong preventive effect of vaccination and early treatment, which minimize the occurrence of infection and subsequent recovery events.

The vaccination campaign under this strategy achieves the highest immunization coverage among all scenarios, elevating the vaccinated child population (V_b) from 0.00 to 2.51×10^7. Consequently, the susceptible children (S_b) slightly decrease from 6.43×10^5 to 3.65×10^5, as the majority are immunized early in the simulation. The environmental viral concentration (C_r) remains at zero, confirming that combined vaccination, treatment, and hygiene interventions effectively suppress pathogen persistence. Among caregivers, the outcomes are equally impressive. The infected caregiver class (I_a) drops completely to 0.00, while the paratenic carriers (P_a) diminish from 6,267.86 to 0.0004. The susceptible caregiver population (S_a) grows substantially from 290.94 to 6,889.99, demonstrating that the integration of education and hygiene measures enhances awareness and reduces transmission risk within the caregiver population. The Figs. 15(a) and 15(b) illustrate the temporal progression of child infections and the corresponding optimal control trajectories under Strategy $\mathbf{S_{15}}$.

Strategy $\mathbf{S_{16}}$ represents the simultaneous application of vaccination, treatment, sanitation, and hygiene interventions, denoted by $u_1(t)$, $u_3(t)$, $u_4(t)$, and $u_5(t)$, respectively, while health education ($u_2(t)$) remains inactive, i.e., ($u_1 \neq 0$, $u_3 \neq 0$, $u_4 \neq 0$, $u_5 \neq 0$, $u_2 = 0$). The simulation results obtained over a 220-day period are summarized in Table 7. Compared with the uncontrolled baseline, Strategy $\mathbf{S_{16}}$ leads to almost complete elimination of rotavirus infections across all population groups. The number of infected children (I_b) decreases from 3.45×10^6 to less than one case (0.10), while hospitalized cases (H_b) fall from 0.00 to 0.03. The recovered class (R_b) reduces from 8.21×10^6 to 5.01×10^3, illustrating the combined effect of vaccination and early treatment in reducing infection and recovery turnover.

The vaccinated population (V_b) rises substantially from 0.00 to 2.51×10^7, with a corresponding decline in susceptible children (S_b) from 6.43×10^5 to 3.65×10^5. The environmental viral concentration (C_r) remains zero, confirming that this strategy effectively halts both transmission and environmental persistence. For caregivers, infection is completely eradicated ($I_a = 0.00$), and paratenic

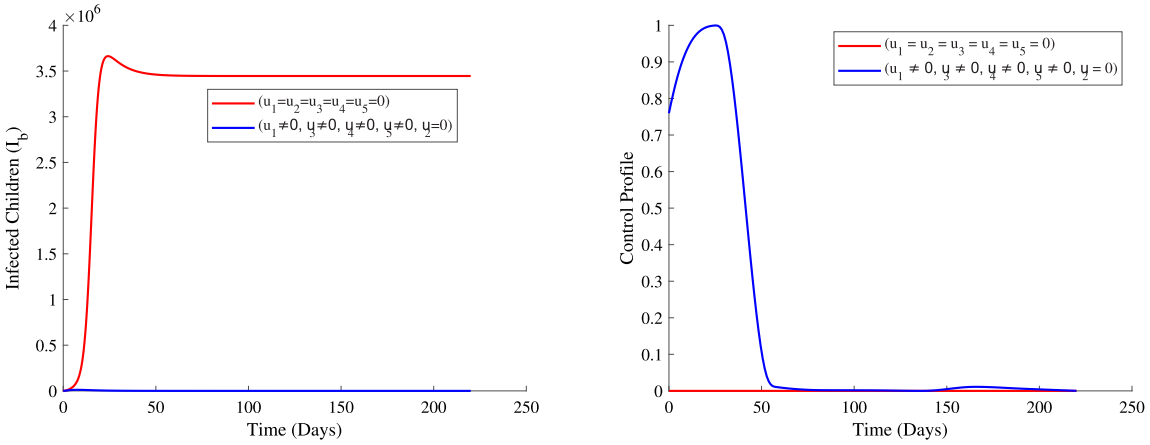

Fig. 16. Temporal dynamics of infected children (left) and optimal control trajectories (right) under Strategy $\mathbf{S_{16}}$ (Vaccination + Treatment + Sanitation + Hygiene).

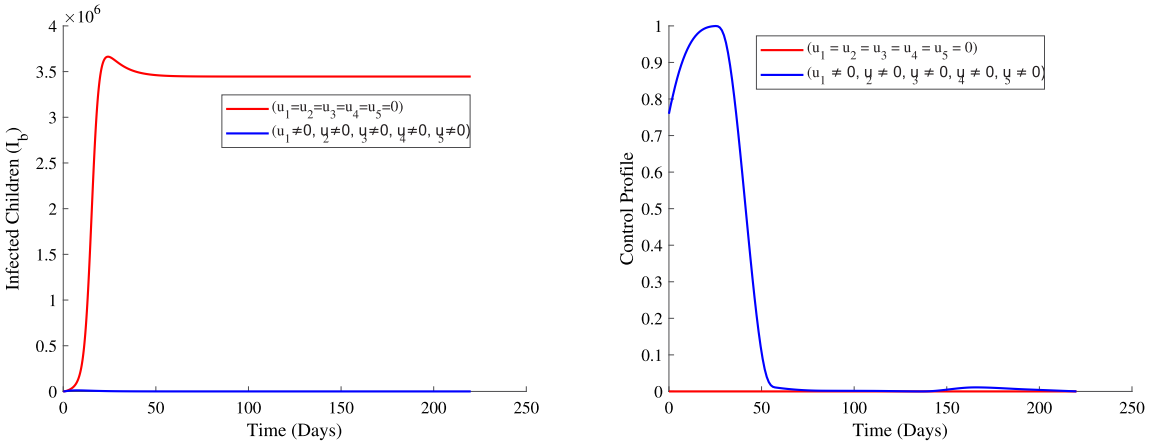

Fig. 17. Temporal dynamics of infected children (left) and optimal control trajectories (right) under strategy $\mathbf{S_{17}}$ (Vaccination + Education + Treatment + Sanitation + Hygiene).

carriers (P_a) decline from 6,267.86 to 0.0005. The susceptible caregiver population (S_a) increases to 6,889.99, indicating a substantial improvement in protection and hygiene outcomes (see Fig. 16).

Strategy $\mathbf{S_{17}}$ involves the simultaneous implementation of vaccination, health education, treatment, sanitation, and hygiene interventions, represented by $u_1(t)$, $u_2(t)$, $u_3(t)$, $u_4(t)$, and $u_5(t)$, respectively. All controls are active, i.e., ($u_1 \neq 0$, $u_2 \neq 0$, $u_3 \neq 0$, $u_4 \neq 0$, $u_5 \neq 0$). Simulation results over 220 days are summarized in Table 7. Compared with the uncontrolled scenario, strategy $\mathbf{S_{17}}$ achieves near-complete elimination of rotavirus infections. Infected children (I_b) decrease from 3.45×10^6 to approximately 0.10, while hospitalized cases (H_b) drop from 0.00 to 0.03. The recovered class (R_b) decreases from 8.21×10^6 to 5.01×10^3, demonstrating the effectiveness of combined vaccination, health education, and treatment.

Vaccinated children (V_b) increase markedly from 0.00 to 2.51×10^7, while susceptible children (S_b) decrease from 6.43×10^5 to 3.65×10^5. Environmental viral concentration (C_r) remains zero, indicating that the intervention effectively suppresses both direct and environmental transmission. For caregivers, infection is completely eliminated ($I_a = 0.00$), paratenic carriers (P_a) decrease from 6,267.86 to 0.0005, and susceptible caregivers (S_a) rise from 290.94 to 6,889.99, reflecting improved protection and hygiene outcomes (see Fig. 17).

Tables 7 and 8 summarize the final outcomes and associated economic measures for the multi-control strategies (S_{13}–S_{17}), each representing a progressive combination of vaccination, education, treatment, sanitation, and hygiene interventions. This integrated presentation facilitates direct comparison of epidemiological performance and cost-efficiency across the combined control approaches.

Table 8 shows that the total implementation costs for combined control strategies (S_{13}–S_{17}) range from approximately \$6.17 × 10^{11} to \$9.15 × 10^{11}. Although these costs are higher than those of other interventions combinations, the associated health benefits are substantially improved, achieving near-complete reductions in child infections for vaccination-inclusive strategies. The cost-effectiveness ratios remain on the order of 10^{17}, indicating that the additional epidemiological gains are attained with acceptable

Table 7
Final population sizes at $T = 220$ days under baseline and combined control strategies (S_{13}–S_{17}).

State variable	No control	S_{13}	S_{14}	S_{15}	S_{16}	S_{17}
Susceptible children (S_b)	643,262.64	364,589.80	11,084,430.01	364,589.80	364,589.80	364,589.80
Vaccinated children (V_b)	0.00	25,079,575.18	318.50	25,079,657.30	25,079,575.18	25,079,575.18
Infected children (I_b)	3,445,717.26	0.10	608,511.84	0.08	0.10	0.10
Hospitalized children (H_b)	0.00	0.03	200,036.41	0.03	0.03	0.03
Recovered children (R_b)	8,207,731.27	5013.06	11,368,201.76	4944.02	5013.06	5013.06
Rotavirus concentration (C_r)	0.00	0.00	0.00	0.00	0.00	0.00
Susceptible caregivers (S_a)	290.94	6889.99	4779.96	6889.99	6889.99	6889.99
Paratenic caregivers (P_a)	6267.86	0.0005	2005.33	0.0004	0.0005	0.0005
Infected caregivers (I_a)	331.20	0.00	104.71	0.00	0.00	0.00

Table 8
Total cost and cost-effectiveness for combined control strategies (S_{13}–S_{17}).

Strategy	Active controls	Total cost ($)	Cost-effectiveness ratio
S_{13}	u_1, u_3, u_5	6.17×10^{11}	1.0×10^{17}
S_{14}	u_2, u_3, u_5	6.35×10^{11}	1.0×10^{17}
S_{15}	u_1, u_2, u_3, u_5	9.15×10^{11}	1.0×10^{17}
S_{16}	u_1, u_3, u_4, u_5	9.15×10^{11}	1.0×10^{17}
S_{17}	u_1, u_2, u_3, u_4, u_5	9.15×10^{11}	1.0×10^{17}

incremental cost. In particular, strategy S_{13}, which combines vaccination, treatment, and hygiene measures, emerges as the most balanced option, providing strong disease suppression at moderate cost. Higher-cost multi-control strategies such as S_{15}–S_{17} achieve full infection elimination but incur greater financial expenditure, highlighting the trade-off between maximal epidemiological impact and economic efficiency.

The results presented in Table 7 demonstrate a consistent epidemiological improvement as more control measures are integrated. Among all the strategies, combined strategy S_{13}, which incorporates vaccination, treatment, and hygiene controls, achieves near-zero infection levels in children and caregivers. This outcome identifies S_{13} as the most epidemiologically impactful intervention, effectively interrupting rotavirus transmission. In contrast, strategies such as S_{14}, which exclude vaccination, record only partial reductions in infections, confirming the critical role of vaccination as the central driver of epidemic control and prevention of new infections. The distribution of vaccinated and susceptible children further supports this conclusion. In vaccination-inclusive strategies, the number of vaccinated individuals rises dramatically (approximately $2.5{\times}10^7$), while the susceptible and infected classes decline sharply. Without vaccination, as seen in S_{14}, the susceptible population remains relatively high and infection persists at moderate levels. Recovery counts also provide important insight: in vaccination and treatment combinations such as S_{13}, recoveries are minimal due to the near elimination of infection, whereas S_{14} registers higher recoveries corresponding to continued but limited disease circulation.

The caregiver population follows a similar pattern. In all strategies that include vaccination (notably S_{13}), caregiver infection is entirely eliminated, demonstrating the indirect protection conferred by child-focused interventions. Environmental contamination remains effectively zero across all strategies that apply sanitation and hygiene controls, indicating the crucial role of environmental hygiene in disrupting transmission pathways. From an economic standpoint, Table 8 reveals total implementation costs ranging between $\$6.17 \times 10^{11}$ and $\$9.15 \times 10^{11}$. Strategy S_{13} provides an optimal balance between cost and epidemiological impact achieving near-total infection elimination at a moderate cost. Although strategies S_{15} to S_{17} involve broader combinations of controls, their higher financial requirements do not substantially improve health outcomes beyond those of S_{13}. In contrast, S_{14}, while comparable in cost, performs significantly worse due to the absence of vaccination. The overall cost-effectiveness analysis, as shown in the histograms, identifies S_{13} as both the most cost-effective and the most impactful strategy, with consistent cost-effectiveness ratios on the order of 10^{17}.

Overall, the comparative assessment confirms that no single control measure alone can achieve complete rotavirus elimination within the simulated period. While individual interventions such as S_3 remain the most economically efficient per case averted, their epidemiological impact is not realized effectively. Integrating multiple interventions markedly enhances both health outcomes and cost-effectiveness. Consequently, strategy S_{13} combining vaccination, treatment, and hygiene emerges as the most practical, sustainable, and impactful option, simultaneously minimizing both control costs and rotavirus infection. The inclusion of additional measures such as education and sanitation may further strengthen long-term rotavirus prevention and public health resilience.

Model discussion and evaluation

Across all seventeen evaluated control strategies (S_1–S_{17}), both epidemiological effectiveness and economic efficiency vary substantially depending on the combination of interventions applied. Single-control strategies (S_1–S_5) generally yield limited reductions in child infections despite considerable costs, with the exception of S_3 (treatment only, u_3), which remains the most cost-effective option in terms of cost per case averted. Combined strategies (S_6–S_{17}) that integrate vaccination (u_1) with other interventions such as treatment (u_3) and hygiene (u_5) demonstrate pronounced reductions in infections and hospitalizations,

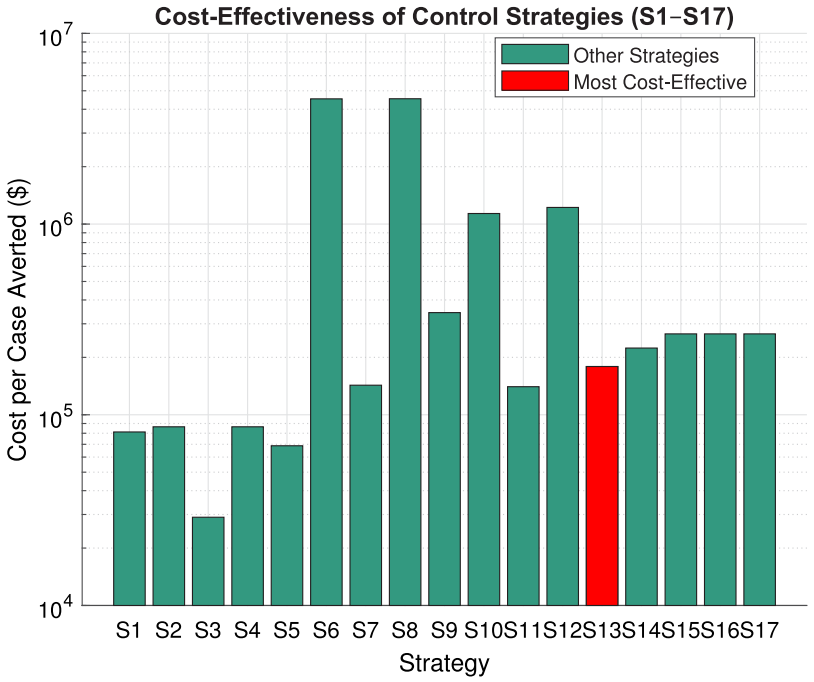

Fig. 18. Cost-effectiveness of control strategies (S_1–S_{17}) expressed as cost per case averted. The most cost-effective strategy (S_{13}) is highlighted in red, while all other strategies are shown in teal. A log scale is used for clarity.

confirming the synergistic benefit of multi-control approaches. For the pediatric population, the most epidemiologically impactful and economically balanced strategy is S_{13}, which combines vaccination, treatment, and hygiene controls. This strategy achieves near-complete elimination of rotavirus infections in children and caregivers at a moderate total cost, making it both highly effective and financially sustainable. Other multi-control strategies, including S_{15}, S_{16}, and S_{17}, also achieve substantial reductions but require higher costs without significant additional benefits, indicating a diminishing return on investment. Conversely, strategies that exclude vaccination, such as S_2, S_4, and S_5, produce negligible epidemiological improvement, underscoring the indispensable role of vaccination in rotavirus control.

Cost analysis indicates that total implementation costs range from approximately $\$2.37 \times 10^{11}$ for single hygiene interventions (S_5) to $\$9.15 \times 10^{11}$ for the full five-control strategy (S_{17}). When evaluating cost-effectiveness (cost per case averted), S_13 clearly stands out as the most efficient strategy, achieving the largest infection reduction at a moderate cost. While S_3 remains the most economical single-control strategy, its epidemiological impact is comparatively limited. High-cost strategies such as S_{14} and S_{17} provide only marginal improvements beyond S_{13}, making them less desirable for real-world implementation. These results emphasize the importance of combining vaccination, treatment, and hygiene to achieve both maximum health impact and optimal cost-effectiveness.

Figs. 18 and 19 collectively illustrate the economic and epidemiological performance of all control strategies. Strategies incorporating vaccination consistently yield the greatest reductions in child infections, with S_{13} demonstrating superior performance in both dimensions. The total cost distribution in Fig. 18 indicates that several minimally effective strategies, such as S_2, S_4, and S_8, are disproportionately costly relative to their benefits, reinforcing the necessity of targeted, evidence-based intervention design. Conversely, S_{13} achieves high infection reduction and strong cost-effectiveness simultaneously, confirming it as the optimal strategy for practical implementation. Therefore, targeted vaccination combined with treatment and hygiene represents the most effective and economically efficient framework for rotavirus elimination. While broader multi-control strategies (S_{15} to S_{17}) achieve comparable epidemiological outcomes, their higher costs limit long-term feasibility. These findings show the importance of integrating essential interventions particularly vaccination while maintaining economic sustainability to maximize public health impact.

Conclusion

In this study, we developed and analyzed a rotavirus transmission model that accounts for the role of child caregivers and evaluates the effectiveness of multiple intervention strategies. The model incorporated controls such as vaccination programs, public health education for caregivers, child healthcare and treatment, improved sanitation and water purification, and hygiene practices for children. Using Lukes' Theorem [43], we established the existence of a unique absolutely continuous solution to the optimal control problem. Specifically, the control system governing rotavirus dynamics is expressed as $\dot{X}(t) = F(t, X(t), U(t))$, with $X(0) = X_0$,

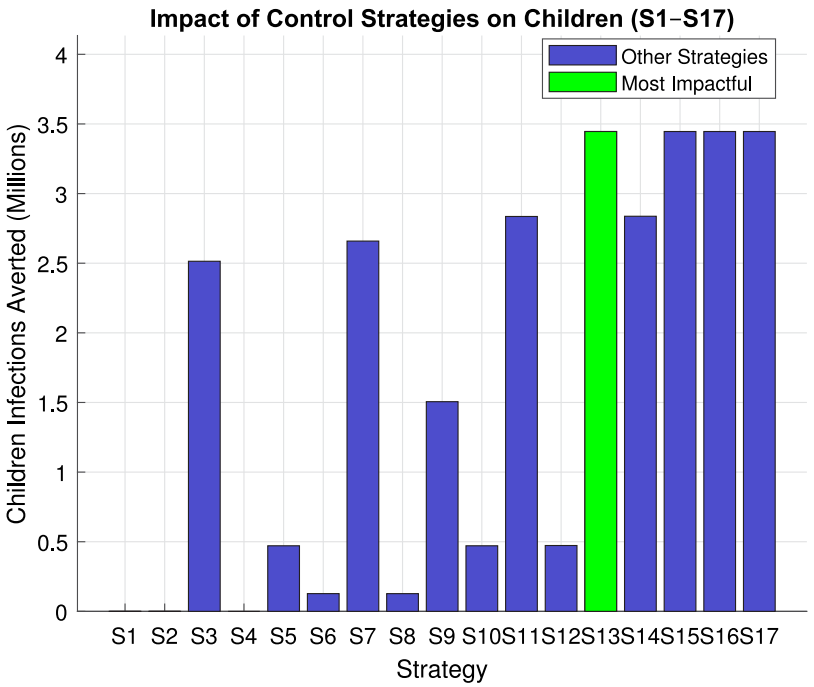

Fig. 19. Epidemiological impact of control strategies (S_1–S_{17}) measured by the number of child infections averted (millions). The strategy achieving the largest reduction (S_{13}) is highlighted in green, while all other strategies are shown in blue.

where $X(t) = (I_b, I_a, H_b, C_r)^\top$ represents the state variables and $U(t) = (u_1, u_2, u_3, u_4, u_5)^\top$ the control functions. The conditions in Eqs. (4)–(7) ensure that a unique solution $X(t)$ exists for all $t \in [0, T]$.

Numerical simulations demonstrated that single-control interventions, such as treatment or hygiene, can reduce infections to some extent, but complete rotavirus suppression requires combined strategies. Among all evaluated interventions, multi-control strategies such as S_{15}, which integrate vaccination, treatment, and hygiene measures, achieved the largest reductions in child infections, effectively approaching elimination. In contrast, the most cost-effective strategy was S_3, focusing on treatment alone, which produced substantial health benefits relative to its lower implementation cost. These findings highlight the trade-off between maximizing epidemiological impact and minimizing resource expenditure, emphasizing that both factors must be considered in public health planning.

The results also indicate the critical role of vaccination in reducing infections among children and indirectly protecting caregivers. Strategies excluding vaccination consistently showed incomplete suppression of disease, with persistent infections among susceptible populations. Environmental sanitation and hygiene measures further contributed to controlling disease transmission by minimizing contamination, while public health education for caregivers enhanced indirect protection by reducing disease transport. Overall, the study gives the importance of a multi-faceted, data-driven approach for rotavirus control. While vaccination serves as a cornerstone of intervention, the combination of treatment, hygiene, and environmental measures maximizes both health outcomes and cost-effectiveness. These findings provide practical guidance for policymakers to allocate resources efficiently and implement interventions that achieve sustainable reductions in rotavirus transmission. Future research should examine the long-term impacts of integrated control strategies and incorporate dynamic factors such as changing population structures and environmental conditions to refine intervention planning further.

CRediT authorship contribution statement

Jeremiah January: Writing – original draft, Conceptualization, Methodology, Formal analysis and Simulation. **Gasper Mwanga:** Methodology, Writing – review & editing, Supervision. **Isack E. Kibona:** Methodology, Formal analysis, Writing – review & editing. **Nyimvua Shaban Mbare:** Formal analysis, Writing – review & editing, Supervision.

Funding

The authors did not receive any funding for this research work.

Declaration of competing interest

The authors declare that they have no known competing financial interests or personal relationships that could have appeared to influence the work reported in this paper.

Data availability

The quantitative data utilized to substantiate the conclusions of this research work have been sourced from previously published articles, and their references as shown in Table 1.

References

[1] Mayo Clinic, Rotavirus Symptoms and Causes, Mayo Clinic presss, 2021.
[2] CDC, Clinical Overview of Rotavirus, MMWR USA, 2024.
[3] WHO, Rotavirus Vaccine Prevetable Diseases Serveillance StandArds, USA, 2018.
[4] D. Kimberlin, M. Brady, M. Jackson, et al., Rotavirus Infections Report of the Committee on Infectious Diseases, 31st ed., American Academy of Pediatrics, 2018.
[5] J. Baker, J. Tate, C. Steiner, et al., Longer-term direct and indirect effects of infant rotavirus vaccination across all ages in the United States in 2000–2013:analysis of a large hospital discharge data set, Clin. Infect. (2019).
[6] M. Bowen, S. Mijatovic-Rustempasic, M. Esona, et al., Rotavirus strain trends during the postlicensure vaccine era: United States, J. Infect. Dis. (2016).
[7] AG. Gichile, Review on the epidemiology of bovine rotavirus and its public health significance, Int J Vet Sci Res 8 (1) (2022) 005–010, dox .doi, org/10.17352/ijvsv.000104 2022.
[8] AP. James, C. Amour, J. Gratz, R. Nshama, T. Walong, B. Mujanga, A. Marco, L. Timothy, Impact of Rotavirus Vaccine Introduction and Postintroduction Etiology of Diarrhea Requiring Hospital Admission in Haydom Tanzania and Rural Africa Setting, Infectious disease Socienty of Americal, USA, 2017.
[9] E.L. Caitlin, A.M. Kelly, Rotavirus, StatPearls Publishing LLC, 2025, https://www.ncbi.nlm.nih.gov/books/NBK558951.
[10] J. Wambui Kibibi, The Role of Oral Rehydration Therapy in Managing Diarrhea in Children. DOI 10.59298/RIJBAS/2024/435862.
[11] R.O. Onyando, Rotavirus Diarrhea Among Young Children before Introduction of the Rotavirus Vaccine Program in Kenya. Baseline Data and Implications for Vaccine Safety Monitoring and Impact Evaluation, Tampere University, Faculty of Social Sciences Finland, 2020.
[12] B.M. Donald, Rotavirus infection: Optimal treatment and prevention, J. Fam. Pr. (2011) 15215, upmc St. margaret, 815 freeport road, pittsburgh.
[13] ANM Kraay, MK. Steele, JM Baker, EW Hall, A Deshpande, A. Saidzosa, et al., Predicting the long-term impact of rotavirus vaccination in 112 countries from 2006–2034:a transmission modeling analysis, 2022, http://dx.doi.org/10.1101/2022.09.23.22280291, medRxiv.
[14] F. Birgitle, F. Elmira, K. Renat, K. Ivar, Dynamic modeling of cost effectivenes of rotavirus vaccination, J. Merging Infect. Dis. (2014) 1–15.
[15] N. Hellen, Livingstone, K. Dmitr, W. Eric, Modeling optimal control of rotavirus disease with different control strategies, J. Math. Comput. Sci. 4 (5) (2014) 892–914.
[16] AL Yustina, S. Nyimvua, M. Goodluck, Modeling optimal control of african trypanosomiasis disease with cost-effective strategies, J. Biol. Systems 29 (4) (2021).
[17] SM Kunwer, D. Vinita, Optimal control of rotavirus infection in breastfed and non-breastfed children, Journal homepage: www.elsevier.com/locate/rico doi:10.1016/j.rico.2024.100452.
[18] E. Leshem, R. Moritz, A. Curns, et al., Rotavirus vaccines and health care utilization for diarrhea in the United States (2007–2011)., Pediatrics 134 (1) (2014) 15–23.
[19] F. Debellut, A. Clark, C. Pecenka, J. Tate, R. Baral, C. Sanderson, U. Parashar, D. Atherly, Evaluating the potential economic and health impact of rotavirus vaccination in 63 middle-income countries not eligible for gavi funding: a modelling study, Lancet Glob Health. 9 (7) (2021) e942–e956, http://dx.doi.org/10.1016/S2214-109X(21)00167-4, Epub 2021 Apr 20. PMID: 33891885; PMCID: PMC8205857.
[20] C. Jordan, ET Jacqueline, P. Umesh, Rotavirus vaccines: progress and new developments, Expert. Opin Biol. Ther. 22 (3) (2022) 423–432, http: //dx.doi.org/10.1080/14712598.2021.1977279.
[21] AO. Amos, OA. Elizabeth, T. Amene, AA. Bukola, CN. Abia, I. Eyoanwan, S. Ify, U. Chizoba, O. Eunice, SA. Sil-Ana, O. Esther, RB. Folasade, OB. Olufunso, et al., Rotavirus surveillance and vaccination in Nigeria: current challenges and important next steps, 2024, https://www.one-health.panafrican-med-journal.com/content/article/13/21/full.
[22] O. Chaturved, L. Eduward, J. Mandu, S. Masupe, Rotavirus diarhoea an analysiss through epidemic modelling, J. Biol. Eng. Inf. http://dx.doi.org/10.5430/ /bei, v4n2p21.
[23] WHO, Global Strategy on People-Centred and Integrated Health Services, Printed by the WHO Document Production Services, Geneva, Switzerland, 2015.
[24] UNHCR Emergency HandBook, Emergency water standard., 2021, https://emergency.unhcr.org.
[25] WHO, Surveillance guide for vaccine-preventable diseases in the WHO south-east Asia region, in: Surveillance Guide for Vaccine-Preventable Diseases in the WHO South-East Asia Region, 2017.
[26] ECDC SCIENTIFIC ADVICE, Expert opinion on rotavirus vaccination in infancy, Eur. Cent. Dis. Prev. Control. (2017).
[27] WHO/IVD/13.08, Introduction of Rotavirus Vaccine, Informatin for Policy Makers, Programe Managers and Health Workers, Genever, 2013.
[28] WH Fleming, RW Rishel, Deterministic and Stochastic Optimal Control, Vol. 1, Springer Science and Business Media, New York, 2012.
[29] B.Z. Aga, M.B. Wolde, S.G. Terefe, Optimal control analysis of smoking dynamics model with cost-effective strategies, J. Appl. Math. Anal. 2025 (2025) 1–17, https://onlinelibrary.wiley.com/doi/10.1155/jama/7486539.
[30] G.A. Berhe, V.N. Sokolov, A.A. Mohamed, Analysis of optimal control strategies for infectious disease models with diffusion, Partial. Differ. Equations Appl. Math. 11 (2024) 100843, http://dx.doi.org/10.1016/j.padiff.2024.100843.
[31] UNICEF, Strategy for Water, Sanitation and Hygiene 2016-2030, New York, 2016.
[32] Charles E Okafor, Obinna I. Ekwunife, Introducing rotavirus vaccine in eight sub-saharan african countries: a cost–benefit analysis, J. Lancet Glob. Health 9 (8) (2021) New York.
[33] Fausta Michael, Mariam M Mirambo, Dafrossa Lyimo, Abdul Salehe, Furaha Kyesi, Delfina R Msanga, Dina Mahamba, Helmut Nyawale, Elizabeth Kwiyolecha, Bernard Okamo, et al., Rotavirus genotype diversity in tanzania during rotavirus vaccine implementation between 2013 and 2018, J. Sci. Rep. 13 (1) (2023) 21795.
[34] E. Bonyan, G. Twagirumukiza, AG. Patience, Mathematical analysis of diarhoea model with saturated incidence rate, Open J. Math. Sci. 2 (2) (2019) 4–9.
[35] I Darti, N.B. Ilmi, A Suryanto, Dynamical analysis of a rotavirus infection model with vaccination and saturation incidence rate, J. Phys. IOP Publ. Conf. Ser. 1562 (1) (2020) 012018.

[36] FA. Adongo, OL. Onyango, J. Bonyo, OG. Lawi, AO. Elisha, A delayed vaccination model for rotavirus infection, Eur. J. Pure Appl. Math. 13.4 13 (4) (2020) Published by New York Business Globalks.
[37] BI. Noraniza, I. Darti, A. Suryanto, Dynamical analysis of a rotavirus infection model with vaccination and saturation incidence rate, J. Phys. Conf. Ser. (2020) http://dx.doi.org/10.1088/1742-6596/1562/1/012018.
[38] N. Nalitolela, Rotavirus Diarrhea Among Children Aged Less than Five Years in Hospital Setting in Dar Es Salaam Tanzania, (Doctoral Dissertation), Muhimbili University of Health and Allied Sciences, Tanzania, 2019.
[39] ES. Sherif, PA. Riyapan, Mathematical Model To Study the Effects of Breastfeeding and Vaccination on Rotavirus Epidemics, Ma thematical Biology Springer- Verlag, 2020.
[40] KS. Mathur, N. Parash, Dynamics of an SVEIRS epidemic model with vaccination and saturated incidence rate, J. Nat. Springer (2018) India.
[41] D. Mahamba, H. Adolfine, F Mashuda, DR Msanga, EC Bendera, EN Kwiyolecha, RB Kidenya, SE Mshana, MM. Mirambo, Prevalence and factors associated with rotavirus infection among vaccinated children hospitalized for acute diarrhea in mwanza city tanzania, Open J. Pediatrics (2020) doi:104236/ojped.2020.103040.
[42] M. Fausta, MM. Mariam, L. Dafrossa, S. Abdul, K. Furaha, et al., Rotavirus genotype diversity in tanzania during rotavirus vaccine implementation between 2013 and 2018, J. Nat. Sci. Rep. (2023) Doi.org/10.1038/s41598-023-49350-4..
[43] D. Lukes, Differential equations: Classical to controlled, in: Mathematics in Science and Engineering, Academic Press, New York, 1982.